POLITECNICO DI TORINO
Repository ISTITUZIONALE

Exponential matrix method for the solution of exact 3D equilibrium equations for free vibrations of functionally graded plates and shells

Original
Exponential matrix method for the solution of exact 3D equilibrium equations for free vibrations of functionally graded plates and shells / Brischetto, Salvatore. - In: JOURNAL OF SANDWICH STRUCTURES AND MATERIALS. - ISSN 1099-6362. - 21:1(2019), pp. 77-114. [10.1177/1099636216686127]

Availability:
This version is available at: 11583/2697400 since: 2020-06-04T00:38:14Z

Publisher:
Sage Publications LTD

Published
DOI:10.1177/1099636216686127

Terms of use:

This article is made available under terms and conditions as specified in the corresponding bibliographic description in the repository

Publisher copyright

(Article begins on next page)

20 April 2024

Check for updates

JOURNAL OF SANDWICH STRUCTURES & MATERIALS

Original Article

Journal of Sandwich Structures and Materials
2019, Vol. 21(1) 77–114
© The Author(s) 2017
Article reuse guidelines:
sagepub.com/journals-permissions
DOI: 10.1177/1099636216686127
journals.sagepub.com/home/jsm
SAGE

Exponential matrix method for the solution of exact 3D equilibrium equations for free vibrations of functionally graded plates and shells

Salvatore Brischetto

Abstract

The present paper analyzes the convergence of the exponential matrix method in the solution of three-dimensional equilibrium equations for the free vibration analysis of functionally graded material structures. The three-dimensional equilibrium equations are written in general orthogonal curvilinear coordinates for one-layered and sandwich plates and shells embedding functionally graded material layers. The resulting system of second-order differential equations is reduced to a system of first-order differential equations redoubling the variables. This system is exactly solved using the exponential matrix method and harmonic displacement components. In the case of functionally graded material plates, the differential equations have variable coefficients because of the material properties which depend on the thickness coordinate z. For functionally graded material shells, the differential equations have variable coefficients because of both changing material properties and curvature terms. Several mathematical layers M can be introduced to approximate the curvature terms and the variable functionally graded material properties to obtain differential equations with constant coefficients. The exponential matrix is applied to solve the resulting system of partial differential equations with constant coefficients, where the used expansion has a very fast convergence ratio. The present work investigates the convergence of the proposed method related to the order N used for the expansion of the exponential matrix and to the number of mathematical layers M used for the approximation of curvature shell terms and variable functionally graded material properties. Both N and M values are analyzed for different geometries, thickness ratios, materials, functionally graded material laws,

Politecnico di Torino, c.so Duca degli Abruzzi 24, Torino, Italy

Corresponding author:
Salvatore Brischetto, Department of Mechanical and Aerospace Engineering, Politecnico di Torino, corso Duca degli Abruzzi, 24, 10129 Torino, Italy.
Email: salvatore.brischetto@polito.it.

lamination sequences, imposed half-wave numbers, frequency orders, and vibration modes.

Keywords
Functionally graded materials, plates and shells, free vibrations and vibration modes, three-dimensional exact solution, exponential matrix method, convergence analysis, mathematical layers, order of expansion for the exponential matrix

Introduction

Functionally graded materials (FGMs) include two or more constituent phases, which have a continuously variable composition [1,2]. FGMs are a new generation of composite materials, and they present a number of advantages such as a potential reduction of in-plane and transverse through-the-thickness stresses, an improved residual stress distribution, higher fracture toughness, reduced stress intensity factors, and enhanced thermal properties [3,4]. In the design of sandwich structures, FGM cores are an interesting alternative to classical cores [5,6]. The use of FGM structures, embedding ceramic and metallic phases, which continuously vary through the thickness direction, could be an optimal solution for thermomechanical problems where severe temperature loads are applied and high-temperature-resistant materials and high structural performances are required [7] (e.g. thermal barrier coatings, engine components, or rocket nozzles). Further FGM applications were described in Mattei et al. [8] where these materials were used to reproduce biological structures characterized by functional spatially distributed gradients in which each layer has one or more specific functions to perform. FGMs require an accurate evaluation of displacements, strains, stresses, and vibrations in order to better execute their assignments. Several two-dimensional (2D) and 3D models have been developed for the analysis of plate and shell elements embedding functionally graded layers.

Plate and shell elements are fundamental in the analysis of single-layered and multilayered structures embedding FGM layers. These elements are defined as two-dimensional and they need an accurate validation to be used with confidence in several engineering fields [9,10]. Two-dimensional elements could be validated and checked by means of 3D exact solutions. Moreover, 3D solutions give further details about 3D behavior and complicating effects introduced by FGM configurations [11,12]. In the literature, exact 3D solutions for FGM structures do not give a general overview of plate and shell elements because they analyze the various geometries separately. The formulation proposed in this paper is general and the equations of motion are written in orthogonal curvilinear coordinates valid for FGM square and rectangular plates, cylindrical shell panels, spherical shell panels, and cylinders. The proposed 3D model exactly solves the equations of

motion in general curvilinear orthogonal coordinates including an exact geometry for shell structures without simplifications. The method uses a layerwise approach, which imposes the continuity of displacements and transverse shear/normal stresses at the interfaces between layers embedded in the multilayered FGM plates and shells. The differential equations are solved by means of the exponential matrix method [13–16], such equations have variable coefficients in the case of shell geometries with curvature terms and/or FGM layers with variable through-the-thickness elastic properties. In these cases, several mathematical layers are introduced to consider constant curvature terms and constant elastic coefficients in the equilibrium equations. Details about the proposed 3D model can be found in past author's works [17–25] where the free vibration analysis of one-layered, multilayered, composite, sandwich and FGM plates, shells and carbon nanotubes is proposed. Similar methods have been used in Messina [26] for the 3D analysis of plates in rectilinear orthogonal coordinates and in Soldatos and Ye [27] for an exact, 3D, free vibration analysis of angle-ply laminated cylinders in cylindrical coordinates. Both works did not consider a general formulation for all the geometries and they did not investigate FGM structures. The present equations of motion written in orthogonal curvilinear coordinates are a general form of the equations of motion written in rectilinear orthogonal coordinates in Messina [26] and in cylindrical coordinates in Soldatos and Ye [27]. The present equations allow general exact solutions for multilayered plate and shell geometries.

In the literature, 3D solutions for FGM structures are developed for specific geometries separately and not in a general framework valid for different cases such as plates, cylindrical, or spherical shells. In a recent work about FGM plates, Dong [28] investigated 3D free vibrations of functionally graded annular plates with different boundary conditions using the Chebyshev–Ritz method. Li et al. [29] used the Chebyshev–Ritz method to analyze free vibrations of functionally graded material sandwich plates. A semi-analytical approach based on differential quadrature method (DQM) and series solution was developed by Malekzadeh [30] to solve the equations of motion for the free vibration analysis of thick FGM plates supported on two-parameter elastic foundation. Three-dimensional models for free vibration analysis of FGM plates based on closed exact solutions can be found in Hosseini-Hashemi [31] and Vel and Batra [32]. Further 3D exact models for FGM plates evaluated the static analysis. Kashtalyan [33] and Xu and Zhou [34] investigated the bending of one-layered functionally graded plates. Kashtalyan and Menshykova [35] proposed the bending analysis of sandwich plates embedding different FGM cores. Zhong and Shang [36] developed an exact 3D analysis for a simply supported and grounded functionally gradient piezoelectric rectangular plate. Other works in the literature were focused on FGM shells. Alibeigloo et al. [37] showed 3D free vibrations of a functionally graded cylindrical shell embedding piezoelectric layers. An analytical and a semi-analytical method were used for simply supported boundary conditions and nonsimply supported boundary conditions, respectively. Zahedinejad et al. [38] used the 3D elasticity theory and the

differential quadrature method to study free vibration analysis of FGM curved thick panels subjected to various boundary conditions. The governing equations were discretized using the trigonometric functions. Chen et al. [39] analyzed free vibrations of simply supported, fluid-filled cylindrically orthotropic functionally graded shells with arbitrary thickness. A laminate approximate model, valid for an arbitrary variation of material properties along the radial direction, was employed. An exact elasticity solution was developed in Vel [40] for the study of forced and free vibrations of functionally graded cylindrical shells. Three-dimensional linear elastodynamics equations were simplified to the case of generalized plane-strain deformation in the axial direction. A meshless method, based on the local Petrov–Galerkin approach, was developed by Sladek et al. [41] in the framework of 3D axisymmetric linear elastic solids with continuously varying material properties for the cases of stress analysis of FGM bodies, heat conduction analysis of FGM bodies [42], and static and elastodynamic analysis of FGM bodies [43].

The 3D equilibrium equations solved in the present paper are written in general orthogonal curvilinear coordinates for the free vibration analysis of FGM single-layered and multilayered plates, cylinders, and cylindrical/spherical shell panels. The solution is proposed in exact form for simply supported structures and harmonic displacement components. The system of second-order partial differential equations is reduced to a system of first-order partial differential equations redoubling the variables. Such differential equations can be solved using the exponential matrix method when constant coefficients are employed. The 3D equilibrium equations have variable coefficients in the case of shells because of the parametric coefficients, which include curvatures and the thickness coordinate z and/or in the case of FGM layers, which present variable elastic coefficients in z. Such equations are simplified in the plate and classical material cases where they show constant coefficients. In the case of a system of partial differential equations with variable coefficients (shell and/or FGM cases), several mathematical layers M, to approximate the curvature terms and the variable elastic coefficients, are introduced to solve the system. Therefore, the exponential matrix can be developed in the thickness direction with an opportune order N. The present paper proposes a convergence analysis for the order N of the exponential matrix and for the number of mathematical layers M in the case of plates and shells embedding different materials included FGMs. This convergence study is proposed for several frequency orders, half-wave numbers, vibration modes, materials, FGM laws, thickness ratios, geometries, and lamination sequences. In the works where this method is described [13–16] or used [17–27], this systematic and thorough study is not contemplated, in particular when FGM layers are included. The proposed convergence analysis for both parameters M and N should be useful to optimize the 3D model in terms of residual error and convergence speed in the case of free vibration analysis of FGM structures. The expansion of the exponential matrix is stable and the method has a very fast convergence. The use of mathematical layers M needs a higher attention.

Geometrical and constitutive equations for FGM structures

The strain–displacement relations of 3D theory of elasticity in orthogonal curvilinear coordinates are developed in Hildebrand et al. [44] and Soedel [45] for the generic k layer of the multilayered shell. In this paper, we consider shells with constant radii of curvature (e.g. cylindrical and spherical geometries). The geometrical relations written for shells with constant radii of curvature are

$$\begin{bmatrix} \epsilon^k_{\alpha\alpha} \\ \epsilon^k_{\beta\beta} \\ \epsilon^k_{zz} \\ \gamma^k_{\beta z} \\ \gamma^k_{\alpha z} \\ \gamma^k_{\alpha\beta} \end{bmatrix} = \begin{bmatrix} \frac{1}{H_\alpha}\frac{\partial}{\partial\alpha} & 0 & \frac{1}{H_\alpha R_\alpha} \\ 0 & \frac{1}{H_\beta}\frac{\partial}{\partial\beta} & \frac{1}{H_\beta R_\beta} \\ 0 & 0 & \frac{\partial}{\partial z} \\ 0 & \left(\frac{\partial}{\partial z} - \frac{1}{H_\beta R_\beta}\right) & \frac{1}{H_\beta}\frac{\partial}{\partial\beta} \\ \left(\frac{\partial}{\partial z} - \frac{1}{H_\alpha R_\alpha}\right) & 0 & \frac{1}{H_\alpha}\frac{\partial}{\partial\alpha} \\ \frac{1}{H_\beta}\frac{\partial}{\partial\beta} & \frac{1}{H_\alpha}\frac{\partial}{\partial\alpha} & 0 \end{bmatrix} \begin{bmatrix} u^k \\ v^k \\ w^k \end{bmatrix} \tag{1}$$

k indicates the generic layer of the multilayer structure and (α, β, z) indicates the curvilinear orthogonal reference system as shown in Figure 1. Symbol ∂ indicates the partial derivatives. The 6×1 vector of strain components $\epsilon^k = \{\epsilon^k_{\alpha\alpha}, \epsilon^k_{\beta\beta}, \epsilon^k_{zz}, \gamma^k_{\beta z}, \gamma^k_{\alpha z}, \gamma^k_{\alpha\beta}\}^T$ is linked with the three displacement components u^k, v^k, and w^k in α, β, and z directions, respectively. R_α and R_β are referred to the mid-surface Ω_0 of the whole multilayered shell (details about notations and reference system for shells are shown in Figure 1). Parametric coefficients H_α and H_β continuously vary through the thickness of the whole multilayered shell and depend on the thickness coordinate

$$\begin{aligned} H_\alpha &= \left(1 + \frac{z}{R_\alpha}\right) = \left(1 + \frac{\tilde{z} - h/2}{R_\alpha}\right), \\ H_\beta &= \left(1 + \frac{z}{R_\beta}\right) = \left(1 + \frac{\tilde{z} - h/2}{R_\beta}\right), \quad H_z = 1 \end{aligned} \tag{2}$$

H_α and H_β depend on the z or $\tilde{z}$ coordinate (see Figure 2 for further details about the coordinate systems). General geometrical relations for spherical shells degenerate into geometrical relations for cylindrical shells when R_α or R_β is infinite (with H_α or H_β equals one), and they degenerate into geometrical relations for plates when both R_α and R_β are infinite (with $H_\alpha = H_\beta = 1$).

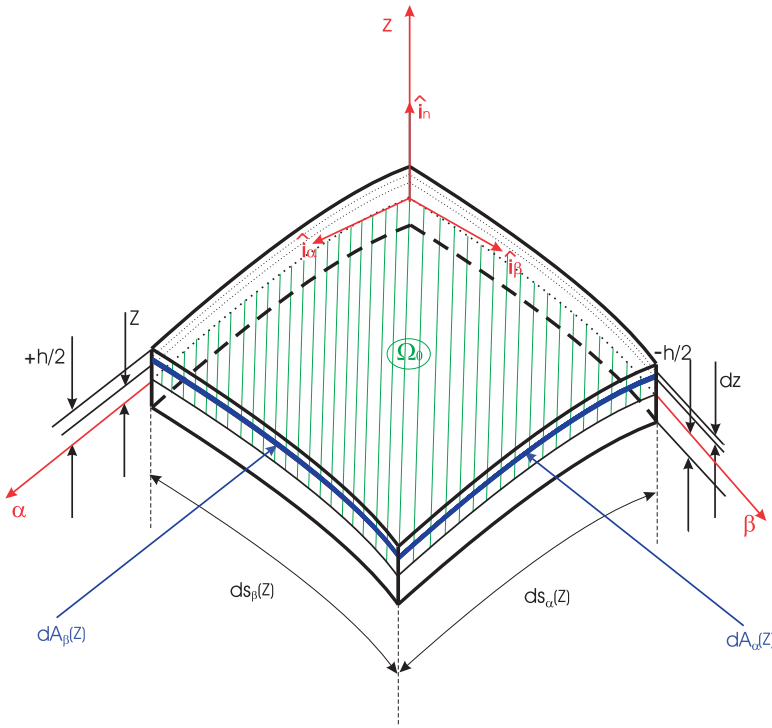

Figure 1. Notations, reference system, and geometrical parameters for shell structures.

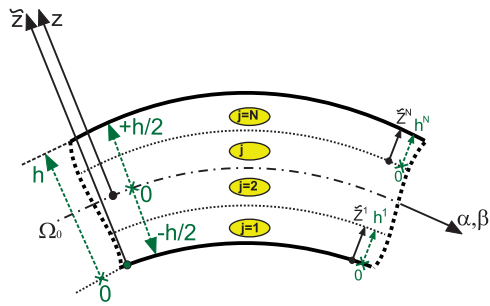

Figure 2. Shell structures, thickness coordinates z and $\tilde{z}$, and reference systems.

The matrix form of the 3D linear elastic isotropic constitutive equations in orthogonal curvilinear coordinates (α, β, z) in the structural reference system is given for a generic k layer of the multilayered FGM structure

$$\boldsymbol{\sigma}^k = \boldsymbol{C}^k(z)\epsilon^k \tag{3}$$

the 6×1 vector of stress components $\boldsymbol{\sigma}^k = \{\sigma^k_{\alpha\alpha}, \sigma^k_{\beta\beta}, \sigma^k_{zz}, \sigma^k_{\beta z}, \sigma^k_{\alpha z}, \sigma^k_{\alpha\beta}\}^T$ is linked with the 6×1 vector of strain components ϵ^k by means of the 6×6 matrix $\boldsymbol{C}^k(z)$ containing the elastic coefficients. Matrix $\boldsymbol{C}^k(z)$ depends on the thickness coordinate z in the case of FGMs because of the variable elastic properties. Details about this matrix can also be found in Reddy [11] and Carrera et al. [12]. The explicit form of $\boldsymbol{C}^k(z)$ is

$$\boldsymbol{C}^k(z) = \begin{bmatrix} C^k_{11}(z) & C^k_{12}(z) & C^k_{13}(z) & 0 & 0 & 0 \\ C^k_{12}(z) & C^k_{22}(z) & C^k_{23}(z) & 0 & 0 & 0 \\ C^k_{13}(z) & C^k_{23}(z) & C^k_{33}(z) & 0 & 0 & 0 \\ 0 & 0 & 0 & C^k_{44}(z) & 0 & 0 \\ 0 & 0 & 0 & 0 & C^k_{55}(z) & 0 \\ 0 & 0 & 0 & 0 & 0 & C^k_{66}(z) \end{bmatrix} \tag{4}$$

Exact 3D equilibrium equations

The three differential equations of equilibrium written for the case of free vibration analysis of multilayered spherical shells made of N_L classical and/or FGM layers with constant radii of curvature R_α and R_β are

$$H_\beta \frac{\partial \sigma^k_{\alpha\alpha}}{\partial \alpha} + H_\alpha \frac{\partial \sigma^k_{\alpha\beta}}{\partial \beta} + H_\alpha H_\beta \frac{\partial \sigma^k_{\alpha z}}{\partial z} + \left(\frac{2H_\beta}{R_\alpha} + \frac{H_\alpha}{R_\beta}\right)\sigma^k_{\alpha z} = \rho^k H_\alpha H_\beta \ddot{u}^k \tag{5}$$

$$H_\beta \frac{\partial \sigma^k_{\alpha\beta}}{\partial \alpha} + H_\alpha \frac{\partial \sigma^k_{\beta\beta}}{\partial \beta} + H_\alpha H_\beta \frac{\partial \sigma^k_{\beta z}}{\partial z} + \left(\frac{2H_\alpha}{R_\beta} + \frac{H_\beta}{R_\alpha}\right)\sigma^k_{\beta z} = \rho^k H_\alpha H_\beta \ddot{v}^k \tag{6}$$

$$\begin{aligned} H_\beta \frac{\partial \sigma^k_{\alpha z}}{\partial \alpha} + H_\alpha \frac{\partial \sigma^k_{\beta z}}{\partial \beta} + H_\alpha H_\beta \frac{\partial \sigma^k_{zz}}{\partial z} - \frac{H_\beta}{R_\alpha}\sigma^k_{\alpha\alpha} - \frac{H_\alpha}{R_\beta}\sigma^k_{\beta\beta} \\ + \left(\frac{H_\beta}{R_\alpha} + \frac{H_\alpha}{R_\beta}\right)\sigma^k_{zz} = \rho^k H_\alpha H_\beta \ddot{w}^k \end{aligned} \tag{7}$$

The most general form for variable radii of curvature can be found in Tornabene [10] and Hildebrand et al. [44]. ρ^k is the mass density depending on the z coordinate in the case of FGMs. $\ddot{u}^k$, $\ddot{v}^k$, and $\ddot{w}^k$ indicate the second temporal derivative of the three displacement components.

Geometrical relations of equation (1) and constitutive equations (3) and (4) are substituted in equations (5) to (7) to obtain a displacement form of the equilibrium

relations. The following form of differential equations of equilibrium is given for a generic classical and/or FGM k layer

$$\begin{aligned}
&\left(-\frac{H_\beta C^k_{55}}{H_\alpha R^2_\alpha}-\frac{C^k_{55}}{R_\alpha R_\beta}\right)u^k+\left(\frac{C^k_{55}H_\beta}{R_\alpha}+\frac{C^k_{55}H_\alpha}{R_\beta}\right)u^k_{,z}+\left(\frac{C^k_{11}H_\beta}{H_\alpha}\right)u^k_{,\alpha\alpha}\\
&\quad+\left(\frac{C^k_{66}H_\alpha}{H_\beta}\right)u^k_{,\beta\beta}+(C^k_{55}H_\alpha H_\beta)u^k_{,zz}+(C^k_{12}+C^k_{66})v^k_{,\alpha\beta}\\
&\quad+\left(\frac{C^k_{11}H_\beta}{H_\alpha R_\alpha}+\frac{C^k_{12}}{R_\beta}+\frac{C^k_{55}H_\beta}{H_\alpha R_\alpha}+\frac{C^k_{55}}{R_\beta}\right)w^k_{,\alpha}\\
&\quad+(C^k_{13}H_\beta+C^k_{55}H_\beta)w^k_{,\alpha z}=\rho^k H_\alpha H_\beta \ddot{u}^k
\end{aligned} \tag{8}$$

$$\begin{aligned}
&\left(-\frac{H_\alpha C^k_{44}}{H_\beta R^2_\beta}-\frac{C^k_{44}}{R_\alpha R_\beta}\right)v^k+\left(\frac{C^k_{44}H_\alpha}{R_\beta}+\frac{C^k_{44}H_\beta}{R_\alpha}\right)v^k_{,z}+\left(\frac{C^k_{66}H_\beta}{H_\alpha}\right)v^k_{,\alpha\alpha}\\
&\quad+\left(\frac{C^k_{22}H_\alpha}{H_\beta}\right)v^k_{,\beta\beta}+(C^k_{44}H_\alpha H_\beta)v^k_{,zz}+(C^k_{12}+C^k_{66})u^k_{,\alpha\beta}\\
&\quad+\left(\frac{C^k_{44}H_\alpha}{H_\beta R_\beta}+\frac{C^k_{44}}{R_\alpha}+\frac{C^k_{22}H_\alpha}{H_\beta R_\beta}+\frac{C^k_{12}}{R_\alpha}\right)w^k_{,\beta}+(C^k_{44}H_\alpha+C^k_{23}H_\alpha)w^k_{,\beta z}=\rho^k H_\alpha H_\beta \ddot{v}^k
\end{aligned} \tag{9}$$

$$\begin{aligned}
&\left(\frac{C^k_{13}}{R_\alpha R_\beta}+\frac{C^k_{23}}{R_\alpha R_\beta}-\frac{C^k_{11}H_\beta}{H_\alpha R^2_\alpha}-\frac{2C^k_{12}}{R_\alpha R_\beta}-\frac{C^k_{22}H_\alpha}{H_\beta R^2_\beta}\right)w^k\\
&\quad+\left(-\frac{C^k_{55}H_\beta}{H_\alpha R_\alpha}+\frac{C^k_{13}}{R_\beta}-\frac{C^k_{11}H_\beta}{H_\alpha R_\alpha}-\frac{C^k_{12}}{R_\beta}\right)u^k_{,\alpha}+\left(-\frac{C^k_{44}H_\alpha}{H_\beta R_\beta}+\frac{C^k_{23}}{R_\alpha}-\frac{C^k_{22}H_\alpha}{H_\beta R_\beta}-\frac{C^k_{12}}{R_\alpha}\right)v^k_{,\beta}\\
&\quad+\left(\frac{C^k_{33}H_\beta}{R_\alpha}+\frac{C^k_{33}H_\alpha}{R_\beta}\right)w^k_{,z}+(C^k_{55}H_\beta+C^k_{13}H_\beta)u^k_{,\alpha z}+(C^k_{44}H_\alpha+C^k_{23}H_\alpha)v^k_{,\beta z}\\
&\quad+\left(C^k_{55}\frac{H_\beta}{H_\alpha}\right)w^k_{,\alpha\alpha}+\left(C^k_{44}\frac{H_\alpha}{H_\beta}\right)w^k_{,\beta\beta}+(C^k_{33}H_\alpha H_\beta)w^k_{,zz}=\rho^k H_\alpha H_\beta \ddot{w}^k
\end{aligned} \tag{10}$$

In equations (8) to (10), elastic coefficients C^k_{qr} and mass density ρ^k are constant for classical materials and depend on the thickness coordinate z ($C^k_{qr}(z)$ and $\rho^k(z)$) for FGMs. R_α and R_β refer to the mid-surface Ω_0 of the multilayered shell. H_α and H_β depend on z coordinate and they are calculated through the thickness of the whole multilayered shell by means of equations (2). Equilibrium relations in equations (8) to (10) are for spherical shell panels, and they automatically degenerate into equilibrium equations for cylindrical closed/open shell panels when R_α or R_β is infinite (with H_α or H_β equals one) and into equilibrium equations for plates when R_α and R_β are infinite (with H_α and H_β equal one). In this way, a unique and general formulation is possible for any geometry. Partial derivatives $\frac{\partial}{\partial\alpha}$, $\frac{\partial}{\partial\beta}$, and $\frac{\partial}{\partial z}$ are indicated with subscripts $_{,\alpha}$, $_{,\beta}$, and $_{,z}$.

The closed form of equations (8) to (10) is developed for simply supported shells and plates when the three displacement components have the following harmonic form

$$u^k(\alpha,\beta,z,t) = U^k(z)e^{i\omega t}\cos(\bar{\alpha}\alpha)\sin(\bar{\beta}\beta) \tag{11}$$

$$v^k(\alpha,\beta,z,t) = V^k(z)e^{i\omega t}\sin(\bar{\alpha}\alpha)\cos(\bar{\beta}\beta) \tag{12}$$

$$w^k(\alpha,\beta,z,t) = W^k(z)e^{i\omega t}\sin(\bar{\alpha}\alpha)\sin(\bar{\beta}\beta) \tag{13}$$

where U^k V^k, and W^k are the displacement amplitudes in α, β, and z directions, respectively. $\omega = 2\pi f$ is the circular frequency where f is the frequency value, t is the time. i is the coefficient of the imaginary unit. In coefficients $\bar{\alpha} = \frac{m\pi}{a}$ and $\bar{\beta} = \frac{n\pi}{b}$, m and n are the half-wave numbers and a and b are the shell dimensions in α and β directions, respectively (calculated at the mid-surface Ω_0).

Equations (11) to (13) are substituted in equations (8) to (10) to obtain the following system

$$\begin{aligned}
&\left(-\frac{C^j_{55}H^j_\beta}{H^j_\alpha R^2_\alpha} - \frac{C^j_{55}}{R_\alpha R_\beta} - \bar{\alpha}^2\frac{C^j_{11}H^j_\beta}{H^j_\alpha} - \bar{\beta}^2\frac{C^j_{66}H^j_\alpha}{H^j_\beta} + \rho^j H^j_\alpha H^j_\beta\omega^2\right)U^j \\
&+(-\bar{\alpha}\bar{\beta}C^j_{12} - \bar{\alpha}\bar{\beta}C^j_{66})V^j + \left(\bar{\alpha}\frac{C^j_{11}H^j_\beta}{H^j_\alpha R_\alpha} + \bar{\alpha}\frac{C^j_{12}}{R_\beta} + \bar{\alpha}\frac{C^j_{55}H^j_\beta}{H^j_\alpha R_\alpha} + \bar{\alpha}\frac{C^j_{55}}{R_\beta}\right)W^j \\
&+\left(\frac{C^j_{55}H^j_\beta}{R_\alpha} + \frac{C^j_{55}H^j_\alpha}{R_\beta}\right)U^j_{,z} + (\bar{\alpha}C^j_{13}H^j_\beta + \bar{\alpha}C^j_{55}H^j_\beta)W^j_{,z} + (C^j_{55}H^j_\alpha H^j_\beta)U^j_{,zz} = 0
\end{aligned} \tag{14}$$

$$\begin{aligned}
&(-\bar{\alpha}\bar{\beta}C^j_{66} - \bar{\alpha}\bar{\beta}C^j_{12})U^j + \left(-\frac{C^j_{44}H^j_\alpha}{H^j_\beta R^2_\beta} - \frac{C^j_{44}}{R_\alpha R_\beta} - \bar{\alpha}^2\frac{C^j_{66}H^j_\beta}{H^j_\alpha} - \bar{\beta}^2\frac{C^j_{22}H^j_\alpha}{H^j_\beta} + \rho^j H^j_\alpha H^j_\beta\omega^2\right)V^j \\
&+\left(\bar{\beta}\frac{C^j_{44}H^j_\alpha}{H^j_\beta R_\beta} + \bar{\beta}\frac{C^j_{44}}{R_\alpha} + \bar{\beta}\frac{C^j_{22}H^j_\alpha}{H^j_\beta R_\beta} + \bar{\beta}\frac{C^j_{12}}{R_\alpha}\right)W^j + \left(\frac{C^j_{44}H^j_\alpha}{R_\beta} + \frac{C^j_{44}H^j_\beta}{R_\alpha}\right)V^j_{,z} \\
&+(\bar{\beta}C^j_{44}H^j_\alpha + \bar{\beta}C^j_{23}H^j_\alpha)W^j_{,z} + (C^j_{44}H^j_\alpha H^j_\beta)V^j_{,zz} = 0
\end{aligned} \tag{15}$$

$$\begin{aligned}
&\left(\bar{\alpha}\frac{C^j_{55}H^j_\beta}{H^j_\alpha R_\alpha} - \bar{\alpha}\frac{C^j_{13}}{R_\beta} + \bar{\alpha}\frac{C^j_{11}H^j_\beta}{H^j_\alpha R_\alpha} + \bar{\alpha}\frac{C^j_{12}}{R_\beta}\right)U^j + \left(\bar{\beta}\frac{C^j_{44}H^j_\alpha}{H^j_\beta R_\beta} - \bar{\beta}\frac{C^j_{23}}{R_\alpha} + \bar{\beta}\frac{C^j_{22}H^j_\alpha}{H^j_\beta R_\beta} + \bar{\beta}\frac{C^j_{12}}{R_\alpha}\right)V^j \\
&+\left(\frac{C^j_{13}}{R_\alpha R_\beta} + \frac{C^j_{23}}{R_\alpha R_\beta} - \frac{C^j_{11}H^j_\beta}{H^j_\alpha R^2_\alpha} - \frac{2C^j_{12}}{R_\alpha R_\beta} - \frac{C^j_{22}H^j_\alpha}{H^j_\beta R^2_\beta} - \bar{\alpha}^2\frac{C^j_{55}H^j_\beta}{H^j_\alpha}\right. \\
&\left.-\bar{\beta}^2\frac{C^j_{44}H^j_\alpha}{H^j_\beta} + \rho^j H^j_\alpha H^j_\beta\omega^2\right)W^j + (-\bar{\alpha}C^j_{55}H^j_\beta - \bar{\alpha}C^j_{13}H^j_\beta)U^j_{,z} + (-\bar{\beta}C^j_{44}H^j_\alpha - \bar{\beta}C^j_{23}H^j_\alpha)V^j_{,z}
\end{aligned}$$

$$+\left(\frac{C_{33}^{j}H_{\beta}^{j}}{R_{\alpha}}+\frac{C_{33}^{j}H_{\alpha}^{j}}{R_{\beta}}\right)W_{,z}^{j}+(C_{33}^{j}H_{\alpha}^{j}H_{\beta}^{j})W_{,zz}^{j}=0. \tag{16}$$

Coefficients in equations (14) to (16), which multiply displacements and their derivatives in z, are not constant in the case of shell geometries and/or FGM layers. Parametric coefficients H_α and H_β depend on the z coordinate (Figure 2) for the shell cases. Elastic coefficients C_{qr} and mass density ρ depend on the z coordinate for the FGM layers. $H_\alpha = H_\beta = 1$ in the case of plate geometry because both radii of curvature R_α and R_β are infinite. C_{qr} and ρ are constant for classical layers. For shell geometries and/or FGM layers, several l mathematical layers are introduced in each k physical layer in order to exactly calculate H_α and H_β, coefficients C_{qr}, and mass density ρ. Coefficients are constant in the l layer because they are evaluated with R_α, R_β, $\bar{\alpha}$, and $\bar{\beta}$ calculated in the mid-surface Ω_0 of the whole shell, and with H_α, H_β, ρ, and C_{qr} calculated in the middle of each l layer. In the present paper, each k physical layer of the multilayered shell is divided in l mathematical layers and the total index for both mathematical and physical layers is $j = k \times l$. Examples for the introduction of j mathematical layers in shell geometries are given in Figures 3 and 4 where a one-layered shell (1 physical layer, $N_L = 1$) and

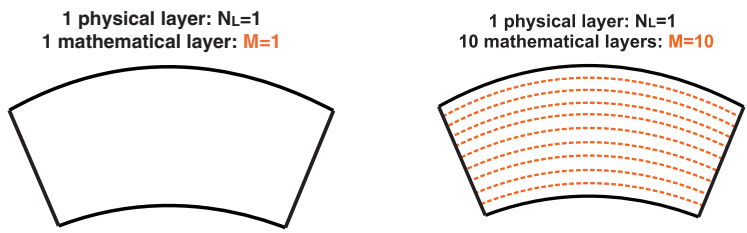

Figure 3. One-layered structures, example for the use of mathematical layers *M*.

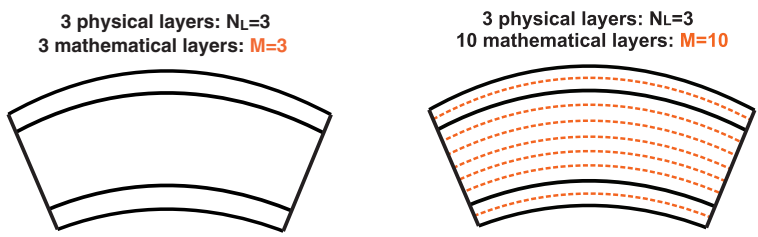

Figure 4. Three-layered structures, example for the use of mathematical layers *M*.

a three-layered shell (3 physical layers, $N_L = 3$), respectively, are divided in $j = M = 10$ mathematical layers.

The system of equations (14) to (16) can be written in a compact form introducing coefficients A_s^j (with s from 1 to 19) for each block in parentheses which multiplies displacement components or their derivatives

$$A_1^j U^j + A_2^j V^j + A_3^j W^j + A_4^j U_{,z}^j + A_5^j W_{,z}^j + A_6^j U_{,zz}^j = 0 \tag{17}$$

$$A_7^j U^j + A_8^j V^j + A_9^j W^j + A_{10}^j V_{,z}^j + A_{11}^j W_{,z}^j + A_{12}^j V_{,zz}^j = 0 \tag{18}$$

$$A_{13}^j U^j + A_{14}^j V^j + A_{15}^j W^j + A_{16}^j U_{,z}^j + A_{17}^j V_{,z}^j + A_{18}^j W_{,z}^j + A_{19}^j W_{,zz}^j = 0. \tag{19}$$

The equations (17) to (19) are a system of three second-order differential equations. They are written for spherical shell panels with constant radii of curvature but they automatically degenerate into equations for cylindrical shells and plates.

The system of second-order differential equations can be reduced to a system of first-order differential equations using the method described in Gustafson [13] and Boyce and DiPrima [14], which redoubles the number of variables. Details about this methodology applied to the proposed equations can be found in Brischetto [18] and [19]. This method allows

$$\begin{bmatrix} A_6^j & 0 & 0 & 0 & 0 & 0 \\ 0 & A_{12}^j & 0 & 0 & 0 & 0 \\ 0 & 0 & A_{19}^j & 0 & 0 & 0 \\ 0 & 0 & 0 & A_6^j & 0 & 0 \\ 0 & 0 & 0 & 0 & A_{12}^j & 0 \\ 0 & 0 & 0 & 0 & 0 & A_{19}^j \end{bmatrix} \begin{bmatrix} U^j \\ V^j \\ W^j \\ U^{j\prime} \\ V^{j\prime} \\ W^{j\prime} \end{bmatrix}' = \begin{bmatrix} 0 & 0 & 0 & A_6^j & 0 & 0 \\ 0 & 0 & 0 & 0 & A_{12}^j & 0 \\ 0 & 0 & 0 & 0 & 0 & A_{19}^j \\ -A_1^j & -A_2^j & -A_3^j & -A_4^j & 0 & -A_5^j \\ -A_7^j & -A_8^j & -A_9^j & 0 & -A_{10}^j & -A_{11}^j \\ -A_{13}^j & -A_{14}^j & -A_{15}^j & -A_{16}^j & -A_{17}^j & -A_{18}^j \end{bmatrix} \begin{bmatrix} U^j \\ V^j \\ W^j \\ U^{j\prime} \\ V^{j\prime} \\ W^{j\prime} \end{bmatrix} \tag{20}$$

Equation (20) can be written in a compact form for a generic j layer

$$\boldsymbol{D}^j \frac{\partial \boldsymbol{U}^j}{\partial \tilde{z}} = \boldsymbol{A}^j \boldsymbol{U}^j \tag{21}$$

where $\frac{\partial \boldsymbol{U}^j}{\partial \tilde{z}} = \boldsymbol{U}^{j\prime}$ and $\boldsymbol{U}^j = [U^j\, V^j\, W^j\, U^{j\prime}\, V^{j\prime}\, W^{j\prime}]$. Equation (21) can be written as

$$\boldsymbol{D}^j \boldsymbol{U}^{j\prime} = \boldsymbol{A}^j \boldsymbol{U}^j \tag{22}$$

$$\boldsymbol{U}^{j\prime} = \boldsymbol{D}^{j-1} \boldsymbol{A}^j\ \boldsymbol{U}^j \tag{23}$$

$$\boldsymbol{U}^{j\prime} = \boldsymbol{A}^{j*}\ \boldsymbol{U}^j \tag{24}$$

with $\boldsymbol{A}^{j*} = \boldsymbol{D}^{j-1}\boldsymbol{A}^j$.

The solution of equation (24) can be written as [14,15]

$$\boldsymbol{U}^j(\tilde{z}^j) = \exp(\boldsymbol{A}^{j*}\tilde{z}^j)\boldsymbol{U}^j(0) \quad \text{with} \quad \tilde{z}^j \in [0, h^j] \tag{25}$$

where $\tilde{z}^j$ is the thickness coordinate of each layer from 0 at the bottom to h^j at the top (Figure 2). The exponential matrix for each j mathematical layer (constant coefficients $\boldsymbol{A}_s^j$) is calculated with $\tilde{z}^j = h^j$

$$\boldsymbol{A}^{j**} = \exp(\boldsymbol{A}^{j*}h^j) = \boldsymbol{I} + \boldsymbol{A}^{j*}h^j + \frac{\boldsymbol{A}^{j*2}}{2!}h^{j2} + \frac{\boldsymbol{A}^{j*3}}{3!}h^{j3} + \cdots + \frac{\boldsymbol{A}^{j*N}}{N!}h^j N \tag{26}$$

where $\boldsymbol{I}$ is the 6×6 identity matrix. This expansion has a fast convergence ratio as indicated in Molery and Van Loan [16] and it is not time consuming from the computational point of view.

$M-1$ transfer matrices $\boldsymbol{T}^{j-1,j}$ must be calculated using for each interface the following conditions for interlaminar continuity of displacements and transverse shear/normal stresses

$$u_b^j = u_t^{j-1}, \quad v_b^j = v_t^{j-1}, \quad w_b^j = w_t^{j-1} \tag{27}$$

$$\sigma_{zzb}^j = \sigma_{zzt}^{j-1}, \quad \sigma_{\alpha zb}^j = \sigma_{\alpha zt}^{j-1}, \quad \sigma_{\beta zb}^j = \sigma_{\beta zt}^{j-1} \tag{28}$$

where displacements and transverse shear/normal stresses at the bottom (b) of the j layer must be equal to displacements and transverse shear/normal stresses at the top (t) of the ($j-1$) layer.

The structures are simply supported and free stresses at the top and at the bottom of the whole multilayered shell, this feature means

$$\sigma_{zz} = \sigma_{\alpha z} = \sigma_{\beta z} = 0 \quad \text{for} \quad z = -h/2, +h/2 \quad \text{or} \quad \tilde{z} = 0, h \tag{29}$$

$$w = v = 0, \quad \sigma_{\alpha\alpha} = 0 \quad \text{for} \quad \alpha = 0, a \tag{30}$$

$$w = u = 0, \quad \sigma_{\beta\beta} = 0 \quad \text{for} \quad \beta = 0, b \tag{31}$$

The use of solution written in equation (26) and the introduction of the conditions summarized in equations (27) and (28) and equations (29) to (31) give a final system written in the following compact form

$$\boldsymbol{E}\ \boldsymbol{U}_1(0) = \boldsymbol{0} \tag{32}$$

All the details about the steps to obtain the final equation (32), omitted in this paper, can be found in past author's works [17–19]. Matrix $\boldsymbol{E}$ has always 6×6 dimension, independently from the employed number of physical and mathematical layers M and even if the method uses a layerwise approach. Each term in the matrix $\boldsymbol{E}$ is a higher order polynomial with an order depending on the value N used for the exponential matrix in equation (26) and on the number of mathematical layers M used in equations (27) and (28). The vector $\boldsymbol{U}_1(0)$ contains the three displacement components and their derivatives with respect z calculated at the bottom ($h^1 = 0$) of the first layer ($j = 1$)

$$\boldsymbol{U}_1(0) = \left[U_1(0) \quad V_1(0) \quad W_1(0) \quad U_1'(0) \quad V_1'(0) \quad W_1'(0) \right]^T \tag{33}$$

The solution is implemented in a Matlab code where only the spherical shell method is included because equations automatically degenerate into cylindrical open/closed shell and plate methods.

The free vibration analysis means to find the nontrivial solution of $\boldsymbol{U}_1(0)$ in equation (32) imposing the determinant of matrix $\boldsymbol{E}$ equals zero

$$det[\boldsymbol{E}] = 0 \tag{34}$$

Equation (34) means to find the roots of an higher order polynomial in $\lambda = \omega^2$. For each pair of half-wave numbers (m,n) a certain number of circular frequencies are obtained depending on the order N chosen for each exponential matrix $\boldsymbol{A}^{j**}$.

Results

This section proposes some benchmarks to evaluate the optimum values for the order of expansion N of the exponential matrix $\boldsymbol{A}^{j**}$ described in equation (26) and for the number of mathematical layers M used in the approximation of the shell curvatures and FGM properties to obtain constant coefficients in 3D equilibrium equations. The M layers are linked by means of the interlaminar continuity conditions proposed in equations (27) and (28).

The geometries, materials, and laminations of proposed benchmarks are summarized in Figures 5 and 6. Figure 5 shows a square plate and a cylindrical shell

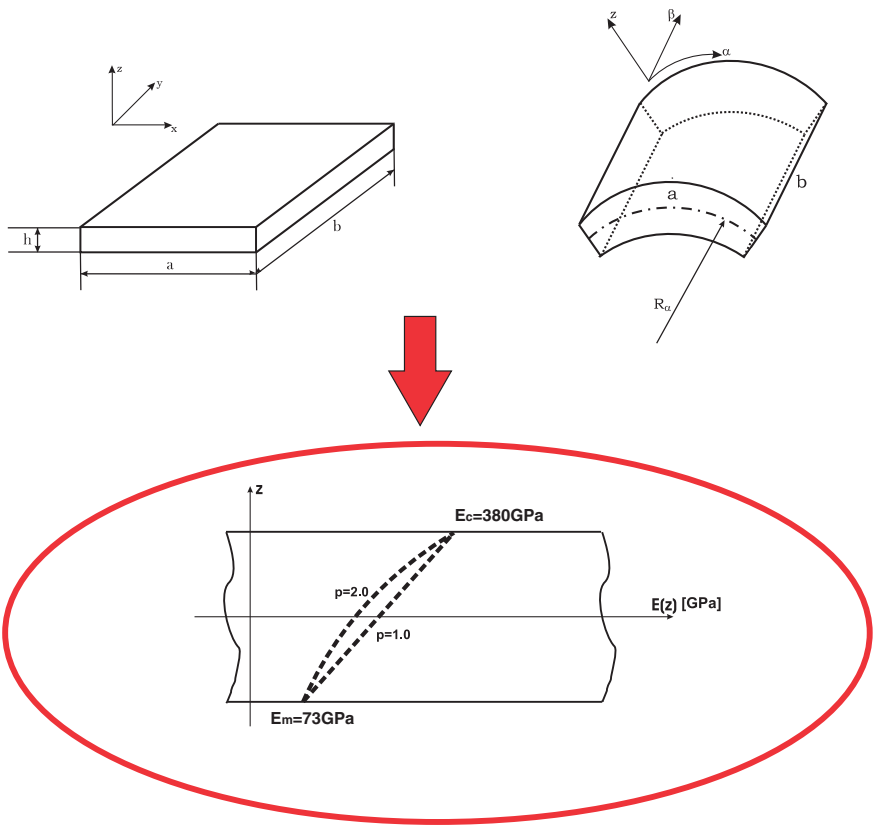

Figure 5. Geometries, laminations, and materials for the analyses in Tables 1 to 8.

panel, both geometries include one FGM layer with two different through-the-thickness laws from the bottom to the top. Figure 6 shows a cylinder and a spherical shell panel, both geometries consider a sandwich configuration with external classical skins and an internal FGM core with two different through-the-thickness laws. All these structures are simply supported. The square plate has global thickness $h = 1$ m. In-plane dimensions are $a = b = 100$ m and $a = b = 5$ m for thickness ratios $a/h = 100$ and $a/h = 5$, respectively. The cylindrical shell has radius of curvature in α-direction $R_\alpha = 10$ m and infinite radius of curvature R_β in β-direction. Cylindrical shell dimensions are a = $\pi/3$ R $_\alpha$ and $b = 20$ m with thickness ratios R_α/h equal 100 and 10. Cylinders have $R_\alpha = 10$ m and an infinite R_β value. Cylinder dimensions are $a = 2\pi R_\alpha$ and $b = 100$ m with thickness ratios R_α/h equal 100 and 10. Spherical shell panel has both radii of curvature $R_\alpha = R_\beta = 10$ m and dimensions $a = b = \pi/3R_\alpha = \pi/3R_\beta$. Investigated thickness ratios R_α/h are 100 and 10.

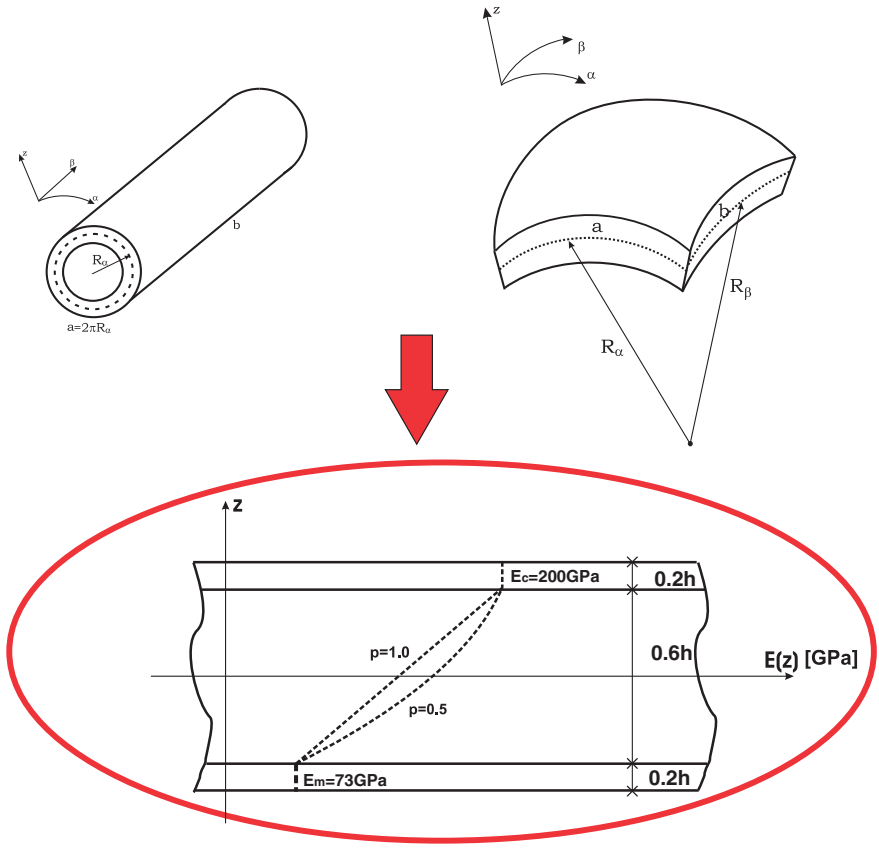

Figure 6. Geometries, laminations, and materials for the analyses in Tables 9 to 16.

The first material configuration is a one-layered FGM structure where the bottom is fully metallic (m) (aluminum alloy Al2024: Young's modulus $E_m = 73$ GPa, mass density $\rho_m = 2800\,\text{kg/m}^3$, and Poisson's ratio $\nu_m = 0.3$) and the top is fully ceramic (c) (alumina Al_2O_3: Young's modulus $E_c = 380$ GPa, mass density $\rho_c = 3800\,\text{kg/m}^3$, and Poisson's ratio $\nu_c = 0.3$). The Poisson's ratio is constant through the thickness. Mass density and Young's modulus vary through the thickness by means of the laws indicated in equations (35) and (36) where the considered volume fraction is proposed in equation (37) for the ceramic (c) phase ($V_c = 0$ at the bottom for $z = -h/2$ and $V_c = 1$ at the top for $z = +h/2$). The exponent p used for the material laws are $p = 1.0$ and 2.0 (Figure 5).

$$E(z) = E_m + (E_c - E_m)V_c \tag{35}$$

$$\rho(z) = \rho_m + (\rho_c - \rho_m)V_c \tag{36}$$

$$V_c = (0.5 + z/h)^p \tag{37}$$

The second material configuration is a sandwich structure with two external skins with a thickness $h_1 = h_3 = 0.2\,\mathrm{h}$ and an internal FGM core with a thickness $h_2 = 0.6\,h$. The bottom skin is metallic (the same aluminum alloy Al2024 already described for the one-layered cases) and the top skin is ceramic (Young's modulus $E_c = 200\,\mathrm{GPa}$, mass density $\rho_c = 5700\,\mathrm{kg/m^3}$, and Poisson's ratio $\nu_c = 0.3$). The functionally graded core has constant Poisson's ratio. Mass density and Young's modulus have the same variation already indicated for the first material configuration in equations (35) to (37). In the calculation of volume fraction V_c the thickness is $h_2 = 0.6\,h$ in place of h, and the thickness coordinate varies from $-0.6\,h/2$ at the bottom to $+0.6\,h/2$ at the top. The p exponents are 0.5 and 1.0.

Results in tables are given as dimensionless circular frequencies $\bar{\omega} = \omega(a/h)^2\sqrt{\rho_c/E_c}$ for plate cases and as $\bar{\omega} = (\omega/10)(R_\alpha/h)^2\sqrt{\rho_c/E_c}$ for shell cases. a is the in-plane dimension of the plate in the α direction, h is the total thickness of the structure, R_α is the radius of curvature in the α direction of shells. ρ_c is the mass density of the ceramic phase, and E_c is the Young's modulus of the ceramic phase. When the half-wave numbers m and n are imposed in the in-plane directions α and β, circular frequencies $\bar{\omega}$ from I, II, III to ∞ are obtained. In the visualization of vibration modes, the thickness coordinate is given in dimensionless form $z^* = z/h$ and the three displacement components are also given in dimensionless form $u^* = u/|U_{max}|$, $v^* = v/|V_{max}|$, and $w^* = w/|W_{max}|$. In proposed tables, the frequencies are indicated in bold when the convergence is reached. The use of NaN indicates "Not a Number" when there is a numerical problem for the solution developed with certain M and N values.

One-layered FGM structures have one physical FGM layer ($N_L = 1$), this layer can be divided in several mathematical layers M. Figure 3 shows the use of 1 and 10 mathematical layers in the one-layered FGM structures. Sandwich structures with isotropic skins and FGM core have three physical layers ($N_L = 3$), these layers can be divided in M uniform mathematical layers. Figure 4 shows a shell structure with three physical layers divided in $M = 10$ mathematical layers. For FGM plates, the use of mathematical layers M is also mandatory, even if the curvature is infinite, because of the variable elastic coefficients.

Tables 1 to 4 show the first three frequencies for the simply supported one-layered FGM plate (thin $a/h = 100$ and thick $a/h = 5$ geometries) when p for the FGM law is equal to 1.0 and 2.0 and the imposed half-wave numbers are $m = n = 1$ and $m = n = 2$. Higher values of mathematical layers M are necessary for $p = 2.0$ with respect to the case $p = 1.0$ (linear through-the-thickness material law) for the same thickness ratio $a/h = 100$ (see comparisons between Table 1 and Table 2). There is also a strong dependence from the imposed half-wave numbers m and n and from the considered mode. The dependency from the thickness ratio is

Table 1. One-layered FGM plate with $p = 1.0$ and $a/h = 100$. First three modes for $m = n = 1$ given as dimensionless circular frequency $\bar{\omega} = \omega(a/h)^2\sqrt{\rho_c/E_c}$. One physical layer ($N_L = 1$) divided in M mathematical layers.

$p = 1.0$; $m = 1$, $n = 1$; $a/h = 100$; I mode

	$N=1$	$N=2$	$N=3$	$N=4$	$N=5$	$N=6$	$N=7$	$N=8$	$N=9$	$N=10$	$N=11$	$N=12$
$M=1$	NaN	8.5676	4.9431	4.9480	4.9470	4.9470	4.9470	4.9470	4.9470	4.9470	4.9643	4.9206
$M=10$	4.5341	7.4535	4.5610	4.5610	4.5610	4.5610	4.5610	4.5610	4.5610	4.5610	4.5610	4.5610
$M=20$	4.5469	4.5682	4.5548	4.5548	4.5548	4.5548	4.5548	4.5548	4.5548	4.5548	4.5548	4.5548
$M=40$	4.5516	4.5566	4.5533	4.5533	4.5533	4.5533	4.5533	4.5533	4.5533	4.5533	4.5533	4.5533
$M=60$	4.5523	4.5545	4.5530	4.5530	4.5530	4.5530	4.5530	4.5530	4.5530	4.5530	4.5530	4.5530
$M=80$	4.5525	4.5537	**4.5529**	**4.5529**	**4.5529**	**4.5529**	**4.5529**	**4.5529**	**4.5529**	**4.5529**	**4.5529**	**4.5529**
$M=100$	4.5526	4.5534	**4.5529**	**4.5529**	**4.5529**	**4.5529**	**4.5529**	**4.5529**	**4.5529**	**4.5529**	**4.5529**	**4.5529**

$p = 1.0$; $m = 1$, $n = 1$; $a/h = 100$; II mode

	$N=1$	$N=2$	$N=3$	$N=4$	$N=5$	$N=6$	$N=7$	$N=8$	$N=9$	$N=10$	$N=11$	$N=12$
$M=1$	NaN	228.27	228.27	228.27	228.27	228.27	228.27	228.27	228.27	228.27	227.05	230.17
$M=10$	228.27	126.79	**228.27**	**228.27**	**228.27**	**228.27**	**228.27**	**228.27**	**228.27**	**228.27**	**228.27**	**228.27**
$M=20$	228.37	**228.27**	**228.27**	**228.27**	**228.27**	**228.27**	**228.27**	**228.27**	**228.27**	**228.27**	**228.27**	**228.27**
$M=40$	**228.27**	**228.27**	**228.27**	**228.27**	**228.27**	**228.27**	**228.27**	**228.27**	**228.27**	**228.27**	**228.27**	**228.27**
$M=60$	**228.27**	**228.27**	**228.27**	**228.27**	**228.27**	**228.27**	**228.27**	**228.27**	**228.27**	**228.27**	**228.27**	**228.27**
$M=80$	**228.27**	**228.27**	**228.27**	**228.27**	**228.27**	**228.27**	**228.27**	**228.27**	**228.27**	**228.27**	**228.27**	**228.27**
$M=100$	**228.27**	**228.27**	**228.27**	**228.27**	**228.27**	**228.27**	**228.27**	**228.27**	**228.27**	**228.27**	**228.27**	**228.27**

$p = 1.0$; $m = 1$, $n = 1$; $a/h = 100$; III mode

	$N=1$	$N=2$	$N=3$	$N=4$	$N=5$	$N=6$	$N=7$	$N=8$	$N=9$	$N=10$	$N=11$	$N=12$
$M=1$	NaN	385.83	385.85	385.85	385.85	385.85	385.85	385.85	385.85	385.85	386.56	384.72
$M=10$	385.84	430.03	**385.84**	**385.84**	**385.84**	**385.84**	**385.84**	**385.84**	**385.84**	**385.84**	**385.84**	**385.84**
$M=20$	385.78	**385.84**	**385.84**	**385.84**	**385.84**	**385.84**	**385.84**	**385.84**	**385.84**	**385.84**	**385.84**	**385.84**
$M=40$	**385.84**	**385.84**	**385.84**	**385.84**	**385.84**	**385.84**	**385.84**	**385.84**	**385.84**	**385.84**	**385.84**	**385.84**
$M=60$	**385.84**	**385.84**	**385.84**	**385.84**	**385.84**	**385.84**	**385.84**	**385.84**	**385.84**	**385.84**	**385.84**	**385.84**
$M=80$	**385.84**	**385.84**	**385.84**	**385.84**	**385.84**	**385.84**	**385.84**	**385.84**	**385.84**	**385.84**	**385.84**	**385.84**
$M=100$	**385.84**	**385.84**	**385.84**	**385.84**	**385.84**	**385.84**	**385.84**	**385.84**	**385.84**	**385.84**	**385.84**	**385.84**

evaluated by means of Tables 3 and 4, which give results for the case $a/h = 5$. In all the discussed tables, when a sufficient number of mathematical layers M is reached to approximate the FGM law, a low value for the order of expansion N of the exponential matrix is requested. $N = 3$ combined with $M = 100$ allow correct results for the first three frequencies investigated in Tables 1 to 4. Figure 7 shows the first

Table 2. One-layered FGM plate with $p = 2.0$ and $a/h = 100$. First three modes for $m = n = 2$ given as dimensionless circular frequency $\bar{\omega} = \omega(a/h)^2\sqrt{\rho_c/E_c}$. One physical layer ($N_L = 1$) divided in M mathematical layers.

$p = 2.0$; $m = 2$, $n = 2$; $a/h = 100$; I mode

	$N=1$	$N=2$	$N=3$	$N=4$	$N=5$	$N=6$	$N=7$	$N=8$	$N=9$	$N=10$	$N=11$	$N=12$
$M=1$	NaN	28.945	16.666	16.732	16.719	16.719	16.719	16.719	16.719	16.719	15.618	17.262
$M=10$	16.446	1211.2	16.542	16.542	16.542	16.542	16.542	16.542	16.542	16.542	16.542	16.542
$M=20$	16.426	16.607	16.559	16.559	16.559	16.559	16.559	16.559	16.559	16.559	16.559	16.559
$M=40$	16.557	16.575	16.563	16.563	16.563	16.563	16.563	16.563	16.563	16.563	16.563	16.563
$M=60$	16.561	16.569	**16.564**	**16.564**	**16.564**	**16.564**	**16.564**	**16.564**	**16.564**	**16.564**	**16.564**	**16.564**
$M=80$	16.563	16.567	**16.564**	**16.564**	**16.564**	**16.564**	**16.564**	**16.564**	**16.564**	**16.564**	**16.564**	**16.564**
$M=100$	16.563	16.566	**16.564**	**16.564**	**16.564**	**16.564**	**16.564**	**16.564**	**16.564**	**16.564**	**16.564**	**16.564**

$p = 2.0$; $m = 2$, $n = 2$; $a/h = 100$; II mode

	$N=1$	$N=2$	$N=3$	$N=4$	$N=5$	$N=6$	$N=7$	$N=8$	$N=9$	$N=10$	$N=11$	$N=12$
$M=1$	NaN	386.14	386.14	386.14	386.14	386.14	386.14	386.14	386.14	386.16	433.76	368.15
$M=10$	411.95	12697	411.95	411.95	411.95	411.95	411.95	411.95	411.95	411.95	411.95	411.95
$M=20$	416.39	412.13	412.13	412.13	412.13	412.13	412.13	412.13	412.13	412.13	412.13	412.13
$M=40$	412.18	412.18	412.18	412.18	412.18	412.18	412.18	412.18	412.18	412.18	412.18	412.18
$M=60$	**412.19**	**412.19**	**412.19**	**412.19**	**412.19**	**412.19**	**412.19**	**412.19**	**412.19**	**412.19**	**412.19**	**412.19**
$M=80$	**412.19**	**412.19**	**412.19**	**412.19**	**412.19**	**412.19**	**412.19**	**412.19**	**412.19**	**412.19**	**412.19**	**412.19**
$M=100$	**412.19**	**412.19**	**412.19**	**412.19**	**412.19**	**412.19**	**412.19**	**412.19**	**412.19**	**412.19**	**412.19**	**412.19**

$p = 2.0$; $m = 2$, $n = 2$; $a/h = 100$; III mode

	$N=1$	$N=2$	$N=3$	$N=4$	$N=5$	$N=6$	$N=7$	$N=8$	$N=9$	$N=10$	$N=11$	$N=12$
$M=1$	NaN	652.57	652.65	652.65	652.65	652.65	652.65	652.65	652.65	652.64	621.92	663.00
$M=10$	696.22	12844	696.22	696.22	696.22	696.22	696.22	696.22	696.22	696.22	696.22	696.22
$M=20$	693.98	696.53	696.53	696.53	696.53	696.53	696.53	696.53	696.53	696.53	696.53	696.53
$M=40$	696.61	696.60	696.61	696.61	696.61	696.61	696.61	696.61	696.61	696.61	696.61	696.61
$M=60$	696.62	696.62	696.62	696.62	696.62	696.62	696.62	696.62	696.62	696.62	696.62	696.62
$M=80$	696.62	696.62	696.62	696.62	696.62	696.62	696.62	696.62	696.62	696.62	696.62	696.62
$M=100$	**696.63**	**696.63**	**696.63**	**696.63**	**696.63**	**696.63**	**696.63**	**696.63**	**696.63**	**696.63**	**696.63**	**696.63**

three vibration modes for the thick ($a/h = 5$) one-layered FGM plate, the case $p = 1.0$ and $m = n = 1$ is proposed on the left side and the case $p = 2.0$ and $m = n = 2$ is proposed on the right side. The convergence of N and M values also depends on the considered mode: simpler vibration modes (e.g. in-plane modes with $w = 0$ and/or through-the-thickness linear displacements) have a fast convergence ratio for the order N and mathematical layers M.

Table 3. One-layered FGM plate with $p = 1.0$ and $a/h = 5$. First three modes for $m = n = 1$ given as dimensionless circular frequency $\bar{\omega} = \omega(a/h)^2\sqrt{\rho_c/E_c}$. One physical layer ($N_L = 1$) divided in M mathematical layers.

$p = 1.0$; $m = 1$, $n = 1$; $a/h = 5$; I mode

	$N=1$	$N=2$	$N=3$	$N=4$	$N=5$	$N=6$	$N=7$	$N=8$	$N=9$	$N=10$	$N=11$	$N=12$
$M=1$	NaN	7.3488	3.0292	4.7187	4.3500	4.4028	4.3931	4.3940	4.3939	4.3939	4.3939	4.3939
$M=10$	4.0851	4.1358	4.0978	4.0979	4.0979	4.0979	4.0979	4.0979	4.0979	4.0979	4.0979	4.0979
$M=20$	4.0904	4.1030	4.0936	4.0936	4.0936	4.0936	4.0936	4.0936	4.0936	4.0936	4.0936	4.0936
$M=40$	4.0918	4.0949	4.0926	4.0926	4.0926	4.0926	4.0926	4.0926	4.0926	4.0926	4.0926	4.0926
$M=60$	4.0920	4.0934	4.0924	4.0924	4.0924	4.0924	4.0924	4.0924	4.0924	4.0924	4.0924	4.0924
$M=80$	4.0921	4.0929	**4.0923**	**4.0923**	**4.0923**	**4.0923**	**4.0923**	**4.0923**	**4.0923**	**4.0923**	**4.0923**	**4.0923**
$M=100$	4.0921	4.0926	**4.0923**	**4.0923**	**4.0923**	**4.0923**	**4.0923**	**4.0923**	**4.0923**	**4.0923**	**4.0923**	**4.0923**

$p = 1.0$; $m = 1$, $n = 1$; $a/h = 5$; II mode

	$N=1$	$N=2$	$N=3$	$N=4$	$N=5$	$N=6$	$N=7$	$N=8$	$N=9$	$N=10$	$N=11$	$N=12$
$M=1$	NaN	11.414	11.414	11.414	11.414	11.414	11.414	11.414	11.414	11.414	11.414	11.414
$M=10$	11.371	11.366	11.369	11.369	11.369	11.369	11.369	11.369	11.369	11.369	11.369	11.369
$M=20$	11.369	**11.368**	**11.368**	**11.368**	**11.368**	**11.368**	**11.368**	**11.368**	**11.368**	**11.368**	**11.368**	**11.368**
$M=40$	**11.368**	**11.368**	**11.368**	**11.368**	**11.368**	**11.368**	**11.368**	**11.368**	**11.368**	**11.368**	**11.368**	**11.368**
$M=60$	**11.368**	**11.368**	**11.368**	**11.368**	**11.368**	**11.368**	**11.368**	**11.368**	**11.368**	**11.368**	**11.368**	**11.368**
$M=80$	**11.368**	**11.368**	**11.368**	**11.368**	**11.368**	**11.368**	**11.368**	**11.368**	**11.368**	**11.368**	**11.368**	**11.368**
$M=100$	**11.368**	**11.368**	**11.368**	**11.368**	**11.368**	**11.368**	**11.368**	**11.368**	**11.368**	**11.368**	**11.368**	**11.368**

$p = 1.0$; $m = 1$, $n = 1$; $a/h = 5$; III mode

	$N=1$	$N=2$	$N=3$	$N=4$	$N=5$	$N=6$	$N=7$	$N=8$	$N=9$	$N=10$	$N=11$	$N=12$
$M=1$	NaN	18.999	19.103	19.178	19.171	19.167	19.168	19.168	19.168	19.168	19.168	19.168
$M=10$	19.040	19.022	19.027	19.027	19.027	19.027	19.027	19.027	19.027	19.027	19.027	19.027
$M=20$	19.029	19.024	**19.026**	**19.026**	**19.026**	**19.026**	**19.026**	**19.026**	**19.026**	**19.026**	**19.026**	**19.026**
$M=40$	19.027	19.025	**19.026**	**19.026**	**19.026**	**19.026**	**19.026**	**19.026**	**19.026**	**19.026**	**19.026**	**19.026**
$M=60$	**19.026**	**19.026**	**19.026**	**19.026**	**19.026**	**19.026**	**19.026**	**19.026**	**19.026**	**19.026**	**19.026**	**19.026**
$M=80$	**19.026**	**19.026**	**19.026**	**19.026**	**19.026**	**19.026**	**19.026**	**19.026**	**19.026**	**19.026**	**19.026**	**19.026**
$M=100$	**19.026**	**19.026**	**19.026**	**19.026**	**19.026**	**19.026**	**19.026**	**19.026**	**19.026**	**19.026**	**19.026**	**19.026**

The one-layered FGM cylindrical shell is investigated in Tables 5 to 8 where the first three frequencies are proposed for different thickness ratios, FGM laws and imposed half-wave numbers m and n. Table 5 shows the thin ($R_\alpha/h = 100$) cylindrical shell with $p = 1.0$ and $m = n = 1$, $M = 20$ mathematical layers combined with $N = 3$ order for the exponential matrix guarantee the convergence for the first three

Table 4. One-layered FGM plate with $p = 2.0$ and $a/h = 5$. First three modes for $m = n = 2$ given as dimensionless circular frequency $\bar{\omega} = \omega(a/h)^2\sqrt{\rho_c/E_c}$. One physical layer ($N_L = 1$) divided in M mathematical layers.

$p = 2.0$; $m = 2$, $n = 2$; $a/h = 5$; I mode

	$N=1$	$N=2$	$N=3$	$N=4$	$N=5$	$N=6$	$N=7$	$N=8$	$N=9$	$N=10$	$N=11$	$N=12$
$M=1$	0.0002	18.738	19.307	14.366	10.364	12.149	11.756	11.845	11.827	11.830	11.829	11.829
$M=10$	11.862	11.854	11.858	11.859	11.859	11.859	11.859	11.859	11.859	11.859	11.859	11.859
$M=20$	11.873	11.891	11.872	11.872	11.872	11.872	11.872	11.872	11.872	11.872	11.872	11.872
$M=40$	11.876	11.880	11.875	11.875	11.875	11.875	11.875	11.875	11.875	11.875	11.875	11.875
$M=60$	11.876	11.878	**11.876**	**11.876**	**11.876**	**11.876**	**11.876**	**11.876**	**11.876**	**11.876**	**11.876**	**11.876**
$M=80$	11.876	11.877	**11.876**	**11.876**	**11.876**	**11.876**	**11.876**	**11.876**	**11.876**	**11.876**	**11.876**	**11.876**
$M=100$	11.876	11.877	**11.876**	**11.876**	**11.876**	**11.876**	**11.876**	**11.876**	**11.876**	**11.876**	**11.876**	**11.876**

$p = 2.0$; $m = 2$, $n = 2$; $a/h = 5$; II mode

	$N=1$	$N=2$	$N=3$	$N=4$	$N=5$	$N=6$	$N=7$	$N=8$	$N=9$	$N=10$	$N=11$	$N=12$
$M=1$	19.307	19.307	30.304	19.307	19.307	19.307	19.307	19.307	19.307	19.307	19.307	19.308
$M=10$	19.975	20.300	19.950	19.951	19.951	19.951	19.951	19.951	19.951	19.951	19.951	19.951
$M=20$	19.960	19.951	19.954	19.954	19.954	19.954	19.954	19.954	19.954	19.954	19.954	19.954
$M=40$	19.956	19.954	**19.955**	**19.955**	**19.955**	**19.955**	**19.955**	**19.955**	**19.955**	**19.955**	**19.955**	**19.955**
$M=60$	19.955	19.954	**19.955**	**19.955**	**19.955**	**19.955**	**19.955**	**19.955**	**19.955**	**19.955**	**19.955**	**19.955**
$M=80$	**19.955**	**19.955**	**19.955**	**19.955**	**19.955**	**19.955**	**19.955**	**19.955**	**19.955**	**19.955**	**19.955**	**19.955**
$M=100$	**19.955**	**19.955**	**19.955**	**19.955**	**19.955**	**19.955**	**19.955**	**19.955**	**19.955**	**19.955**	**19.955**	**19.955**

$p = 2.0$; $m = 2$, $n = 2$; $a/h = 5$; III mode

	$N=1$	$N=2$	$N=3$	$N=4$	$N=5$	$N=6$	$N=7$	$N=8$	$N=9$	$N=10$	$N=11$	$N=12$
$M=1$	32.634	31.253	32.877	31.087	31.925	31.626	31.554	31.578	31.583	31.582	31.581	31.579
$M=10$	31.825	30.538	31.595	31.597	31.597	31.597	31.597	31.597	31.597	31.597	31.597	31.597
$M=20$	31.652	31.569	31.592	31.592	31.592	31.592	31.592	31.592	31.592	31.592	31.592	31.592
$M=40$	31.606	31.586	**31.591**	**31.591**	**31.591**	**31.591**	**31.591**	**31.591**	**31.591**	**31.591**	**31.591**	**31.591**
$M=60$	31.598	31.588	**31.591**	**31.591**	**31.591**	**31.591**	**31.591**	**31.591**	**31.591**	**31.591**	**31.591**	**31.591**
$M=80$	31.595	31.590	**31.591**	**31.591**	**31.591**	**31.591**	**31.591**	**31.591**	**31.591**	**31.591**	**31.591**	**31.591**
$M=100$	31.593	31.590	**31.591**	**31.591**	**31.591**	**31.591**	**31.591**	**31.591**	**31.591**	**31.591**	**31.591**	**31.591**

frequencies. Table 6 considers the same thickness ratio with $p = 2.0$ for the FGM law and $m = n = 2$ half-wave numbers. When the FGM law is not linear in z, higher values for the number of mathematical layers M is requested. In this case $M = 100$ combined with $N = 2$ always give correct results for the first three frequencies. Tables 7 and 8 propose the same cases seen in Tables 5 to 6 but for a thick shell

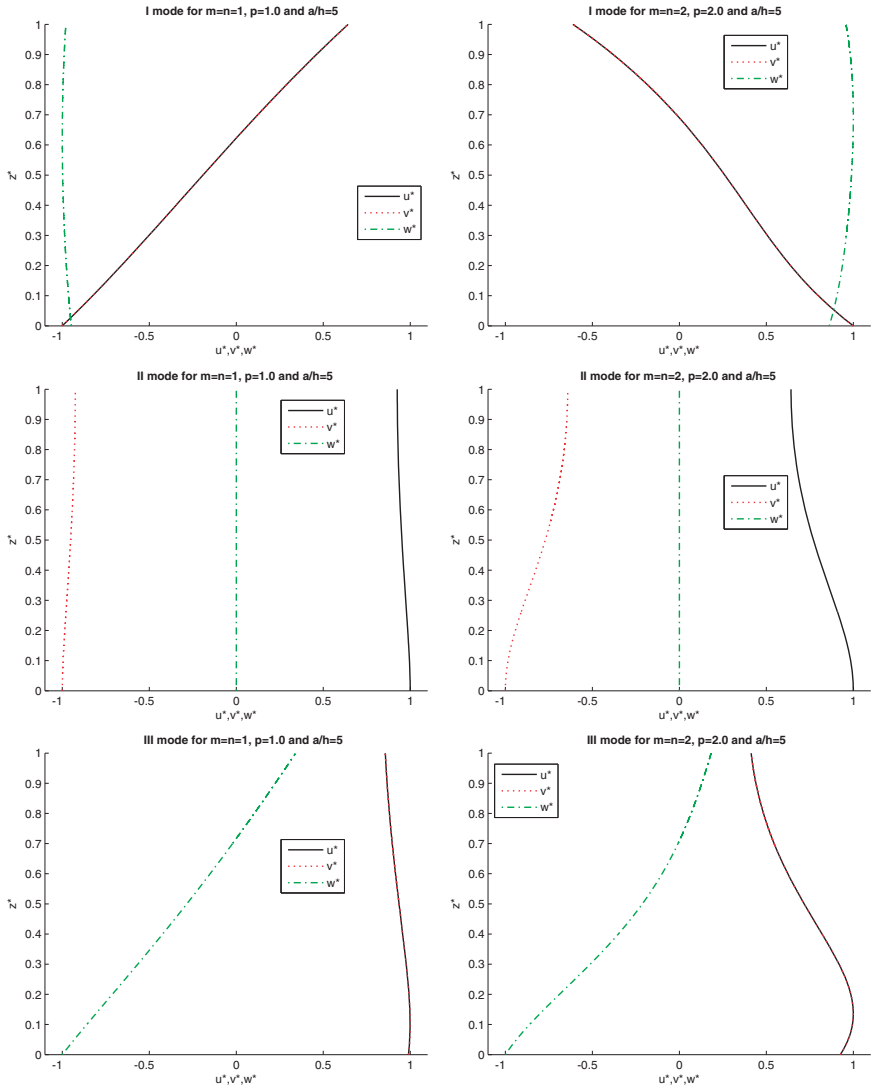

Figure 7. First three vibration modes for one-layered FGM plate ($a/h = 5$) for $p = 1.0$ and 2.0 and $m = n = 1$ and $m = n = 2$.

($R_\alpha/h = 10$ in place of $R_\alpha/h = 100$). The dependence of M and N values from the p coefficient of the FGM law is stronger than the dependence from the thickness ratio. In conclusion, $N = 3$ combined with $M = 100$ give a correct convergence of the method as already seen for the plate case. It is important to notice that in the shell cases, the M mathematical layers are used to approximate both curvature

Table 5. One-layered FGM cylindrical shell with $p = 1.0$ and $R_\alpha/h = 100$. First three modes for $m = n = 1$ given as dimensionless circular frequency $\bar{\omega} = (\omega/10)(R_\alpha/h)^2\sqrt{\rho_c/E_c}$. One physical layer ($N_L = 1$) divided in M mathematical layers.

$p = 1.0$; $m = 1$, $n = 1$; $R_\alpha/h = 100$; I mode

	$N=1$	$N=2$	$N=3$	$N=4$	$N=5$	$N=6$	$N=7$	$N=8$	$N=9$	$N=10$	$N=11$	$N=12$
$M=1$	7.7438	17.428	17.021	17.025	17.025	17.025	17.025	17.025	17.025	17.025	17.025	17.025
$M=10$	16.314	16.986	16.982	16.982	16.982	16.982	16.982	16.982	16.982	16.982	16.982	16.982
$M=20$	16.651	16.982	**16.981**	**16.981**	**16.981**	**16.981**	**16.981**	**16.981**	**16.981**	**16.981**	**16.981**	**16.981**
$M=40$	16.817	**16.981**	**16.981**	**16.981**	**16.981**	**16.981**	**16.981**	**16.981**	**16.981**	**16.981**	**16.981**	**16.981**
$M=60$	16.872	**16.981**	**16.981**	**16.981**	**16.981**	**16.981**	**16.981**	**16.981**	**16.981**	**16.981**	**16.981**	**16.981**
$M=80$	16.899	**16.981**	**16.981**	**16.981**	**16.981**	**16.981**	**16.981**	**16.981**	**16.981**	**16.981**	**16.981**	**16.981**
$M=100$	16.916	**16.981**	**16.981**	**16.981**	**16.981**	**16.981**	**16.981**	**16.981**	**16.981**	**16.981**	**16.981**	**16.981**

$p = 1.0$; $m = 1$, $n = 1$; $R_\alpha/h = 100$; II mode

	$N=1$	$N=2$	$N=3$	$N=4$	$N=5$	$N=6$	$N=7$	$N=8$	$N=9$	$N=10$	$N=11$	$N=12$
$M=1$	178.57	178.63	178.63	178.63	178.63	178.63	178.63	178.63	178.63	178.63	178.63	178.63
$M=10$	178.56	**178.57**	**178.57**	**178.57**	**178.57**	**178.57**	**178.57**	**178.57**	**178.57**	**178.57**	**178.57**	**178.57**
$M=20$	178.56	**178.57**	**178.57**	**178.57**	**178.57**	**178.57**	**178.57**	**178.57**	**178.57**	**178.57**	**178.57**	**178.57**
$M=40$	**178.57**	**178.57**	**178.57**	**178.57**	**178.57**	**178.57**	**178.57**	**178.57**	**178.57**	**178.57**	**178.57**	**178.57**
$M=60$	**178.57**	**178.57**	**178.57**	**178.57**	**178.57**	**178.57**	**178.57**	**178.57**	**178.57**	**178.57**	**178.57**	**178.57**
$M=80$	**178.57**	**178.57**	**178.57**	**178.57**	**178.57**	**178.57**	**178.57**	**178.57**	**178.57**	**178.57**	**178.57**	**178.57**
$M=100$	**178.57**	**178.57**	**178.57**	**178.57**	**178.57**	**178.57**	**178.57**	**178.57**	**178.57**	**178.57**	**178.57**	**178.57**

$p = 1.0$; $m = 1$, $n = 1$; $R_\alpha/h = 100$; III mode

	$N=1$	$N=2$	$N=3$	$N=4$	$N=5$	$N=6$	$N=7$	$N=8$	$N=9$	$N=10$	$N=11$	$N=12$
$M=1$	303.22	303.49	303.50	303.50	303.50	303.50	303.50	303.50	303.50	303.50	303.50	303.50
$M=10$	303.64	303.66	303.66	303.66	303.66	303.66	303.66	303.66	303.66	303.66	303.66	303.66
$M=20$	303.65	**303.67**	**303.67**	**303.67**	**303.67**	**303.67**	**303.67**	**303.67**	**303.67**	**303.67**	**303.67**	**303.67**
$M=40$	303.66	**303.67**	**303.67**	**303.67**	**303.67**	**303.67**	**303.67**	**303.67**	**303.67**	**303.67**	**303.67**	**303.67**
$M=60$	303.66	**303.67**	**303.67**	**303.67**	**303.67**	**303.67**	**303.67**	**303.67**	**303.67**	**303.67**	**303.67**	**303.67**
$M=80$	303.66	**303.67**	**303.67**	**303.67**	**303.67**	**303.67**	**303.67**	**303.67**	**303.67**	**303.67**	**303.67**	**303.67**
$M=100$	303.66	**303.67**	**303.67**	**303.67**	**303.67**	**303.67**	**303.67**	**303.67**	**303.67**	**303.67**	**303.67**	**303.67**

terms and FGM laws. In the plate case, the M mathematical layers are mandatory only for the FGM law approximation because these geometries do not request any curvature approximation.

The first three frequencies for a sandwich cylinder with FGM core and classical skins (full metallic at the bottom and full ceramic at the top) are investigated in

Table 6. One-layered FGM cylindrical shell with $p = 2.0$ and $R_\alpha/h = 100$. First three modes for $m = n = 2$ given as dimensionless circular frequency $\bar{\omega} = (\omega/10)(R_\alpha/h)^2\sqrt{\rho_c/E_c}$. One physical layer ($N_L = 1$) divided in M mathematical layers.

$p = 2.0$; $m = 2$, $n = 2$; $R_\alpha/h = 100$; I mode

	$N=1$	$N=2$	$N=3$	$N=4$	$N=5$	$N=6$	$N=7$	$N=8$	$N=9$	$N=10$	$N=11$	$N=12$
$M=1$	NaN	22.247	17.570	17.626	17.623	17.623	17.623	17.623	17.623	17.623	17.623	17.623
$M=10$	15.678	18.393	18.337	18.337	18.337	18.337	18.337	18.337	18.337	18.337	18.337	18.337
$M=20$	17.077	18.361	18.347	18.347	18.347	18.347	18.347	18.347	18.347	18.347	18.347	18.347
$M=40$	17.728	18.353	18.350	18.350	18.350	18.350	18.350	18.350	18.350	18.350	18.350	18.350
$M=60$	17.938	18.352	18.350	18.350	18.350	18.350	18.350	18.350	18.350	18.350	18.350	18.350
$M=80$	18.043	18.351	18.350	18.350	18.350	18.350	18.350	18.350	18.350	18.350	18.350	18.350
$M=100$	18.105	**18.351**	**18.351**	**18.351**	**18.351**	**18.351**	**18.351**	**18.351**	**18.351**	**18.351**	**18.351**	**18.351**

$p = 2.0$; $m = 2$, $n = 2$; $R_\alpha/h = 100$; II mode

	$N=1$	$N=2$	$N=3$	$N=4$	$N=5$	$N=6$	$N=7$	$N=8$	$N=9$	$N=10$	$N=11$	$N=12$
$M=1$	NaN	296.44	296.43	296.43	296.43	296.43	296.43	296.43	296.43	296.43	296.43	296.43
$M=10$	316.15	316.15	316.15	316.15	316.15	316.15	316.15	316.15	316.15	316.15	316.15	316.15
$M=20$	316.29	316.29	316.29	316.29	316.29	316.29	316.29	316.29	316.29	316.29	316.29	316.29
$M=40$	316.32	316.33	316.33	316.33	316.33	316.33	316.33	316.33	316.33	316.33	316.33	316.33
$M=60$	316.33	316.33	316.33	316.33	316.33	316.33	316.33	316.33	316.33	316.33	316.33	316.33
$M=80$	316.33	316.33	316.33	316.33	316.33	316.33	316.33	316.33	316.33	316.33	316.33	316.33
$M=100$	**316.34**	**316.34**	**316.34**	**316.34**	**316.34**	**316.34**	**316.34**	**316.34**	**316.34**	**316.34**	**316.34**	**316.34**

$p = 2.0$; $m = 2$, $n = 2$; $R_\alpha/h = 100$; III mode

	$N=1$	$N=2$	$N=3$	$N=4$	$N=5$	$N=6$	$N=7$	$N=8$	$N=9$	$N=10$	$N=11$	$N=12$
$M=1$	NaN	501.35	501.39	501.39	501.39	501.39	501.39	501.39	501.39	501.39	501.39	501.39
$M=10$	535.35	535.38	535.38	535.38	535.38	535.38	535.38	535.38	535.38	535.38	535.38	535.38
$M=20$	535.61	535.63	535.63	535.63	535.63	535.63	535.63	535.63	535.63	535.63	535.63	535.63
$M=40$	535.68	535.69	535.69	535.69	535.69	535.69	535.69	535.69	535.69	535.69	535.69	535.69
$M=60$	535.69	**535.70**	**535.70**	**535.70**	**535.70**	**535.70**	**535.70**	**535.70**	**535.70**	**535.70**	**535.70**	**535.70**
$M=80$	**535.70**	**535.70**	**535.70**	**535.70**	**535.70**	**535.70**	**535.70**	**535.70**	**535.70**	**535.70**	**535.70**	**535.70**
$M=100$	**535.70**	**535.70**	**535.70**	**535.70**	**535.70**	**535.70**	**535.70**	**535.70**	**535.70**	**535.70**	**535.70**	**535.70**

Tables 9 to 12 considering thin ($R_\alpha/h = 100$) and thick ($R_\alpha/h = 10$) geometries. FGM law exponents p are equal to 1.0 and 0.5, and couples of half-wave numbers are ($m = 2$, $n = 1$) and ($m = 2$, $n = 2$). The closed geometry of the cylinder gives a geometrical symmetry and a high value of rigidity. For these two reasons, smaller number M of mathematical layers are requested if compared with the same cases

Table 7. One-layered FGM cylindrical shell with $p = 1.0$ and $R_\alpha/h = 10$. First three modes for $m = n = 1$ given as dimensionless circular frequency $\bar{\omega} = (\omega/10)(R_\alpha/h)^2\sqrt{\rho_c/E_c}$. One physical layer ($N_L = 1$) divided in M mathematical layers.

$p = 1.0$; $m = 1$, $n = 1$; $R_\alpha/h = 10$; I mode

	$N=1$	$N=2$	$N=3$	$N=4$	$N=5$	$N=6$	$N=7$	$N=8$	$N=9$	$N=10$	$N=11$	$N=12$
$M=1$	NaN	0.5040	0.2729	0.3093	0.3053	0.3055	0.3055	0.3055	0.3055	0.3055	0.3055	0.3055
$M=10$	0.2353	0.2787	0.2764	0.2765	0.2765	0.2765	0.2765	0.2765	0.2765	0.2765	0.2765	0.2765
$M=20$	0.2567	0.2767	0.2761	0.2761	0.2761	0.2761	0.2761	0.2761	0.2761	0.2761	0.2761	0.2761
$M=40$	0.2666	0.2762	**0.2760**	**0.2760**	**0.2760**	**0.2760**	**0.2760**	**0.2760**	**0.2760**	**0.2760**	**0.2760**	**0.2760**
$M=60$	0.2698	0.2761	**0.2760**	**0.2760**	**0.2760**	**0.2760**	**0.2760**	**0.2760**	**0.2760**	**0.2760**	**0.2760**	**0.2760**
$M=80$	0.2713	**0.2760**	**0.2760**	**0.2760**	**0.2760**	**0.2760**	**0.2760**	**0.2760**	**0.2760**	**0.2760**	**0.2760**	**0.2760**
$M=100$	0.2723	**0.2760**	**0.2760**	**0.2760**	**0.2760**	**0.2760**	**0.2760**	**0.2760**	**0.2760**	**0.2760**	**0.2760**	**0.2760**

$p = 1.0$; $m = 1$, $n = 1$; $R_\alpha/h = 10$; II mode

	$N=1$	$N=2$	$N=3$	$N=4$	$N=5$	$N=6$	$N=7$	$N=8$	$N=9$	$N=10$	$N=11$	$N=12$
$M=1$	NaN	1.7925	1.7877	1.7881	1.7881	1.7881	1.7881	1.7881	1.7881	1.7881	1.7881	1.7881
$M=10$	1.7795	1.7799	1.7800	1.7800	1.7800	1.7800	1.7800	1.7800	1.7800	1.7800	1.7800	1.7800
$M=20$	1.7797	**1.7799**	**1.7799**	**1.7799**	**1.7799**	**1.7799**	**1.7799**	**1.7799**	**1.7799**	**1.7799**	**1.7799**	**1.7799**
$M=40$	1.7798	**1.7799**	**1.7799**	**1.7799**	**1.7799**	**1.7799**	**1.7799**	**1.7799**	**1.7799**	**1.7799**	**1.7799**	**1.7799**
$M=60$	1.7798	**1.7799**	**1.7799**	**1.7799**	**1.7799**	**1.7799**	**1.7799**	**1.7799**	**1.7799**	**1.7799**	**1.7799**	**1.7799**
$M=80$	1.7798	**1.7799**	**1.7799**	**1.7799**	**1.7799**	**1.7799**	**1.7799**	**1.7799**	**1.7799**	**1.7799**	**1.7799**	**1.7799**
$M=100$	1.7798	**1.7799**	**1.7799**	**1.7799**	**1.7799**	**1.7799**	**1.7799**	**1.7799**	**1.7799**	**1.7799**	**1.7799**	**1.7799**

$p = 1.0$; $m = 1$, $n = 1$; $R_\alpha/h = 10$; III mode

	$N=1$	$N=2$	$N=3$	$N=4$	$N=5$	$N=6$	$N=7$	$N=8$	$N=9$	$N=10$	$N=11$	$N=12$
$M=1$	NaN	3.0206	3.0312	3.0307	3.0305	3.0306	3.0306	3.0306	3.0306	3.0306	3.0306	3.0305
$M=10$	3.0388	3.0413	3.0414	3.0414	3.0414	3.0414	3.0414	3.0414	3.0414	3.0414	3.0414	3.0414
$M=20$	3.0401	**3.0415**	**3.0415**	**3.0415**	**3.0415**	**3.0415**	**3.0415**	**3.0415**	**3.0415**	**3.0415**	**3.0415**	**3.0415**
$M=40$	3.0408	**3.0415**	**3.0415**	**3.0415**	**3.0415**	**3.0415**	**3.0415**	**3.0415**	**3.0415**	**3.0415**	**3.0415**	**3.0415**
$M=60$	3.0411	**3.0415**	**3.0415**	**3.0415**	**3.0415**	**3.0415**	**3.0415**	**3.0415**	**3.0415**	**3.0415**	**3.0415**	**3.0415**
$M=80$	3.0412	**3.0415**	**3.0415**	**3.0415**	**3.0415**	**3.0415**	**3.0415**	**3.0415**	**3.0415**	**3.0415**	**3.0415**	**3.0415**
$M=100$	3.0412	**3.0415**	**3.0415**	**3.0415**	**3.0415**	**3.0415**	**3.0415**	**3.0415**	**3.0415**	**3.0415**	**3.0415**	**3.0415**

seen for one-layered FGM cylindrical shell panels and sandwich FGM spherical shell panels. However, the case with the exponent $p = 0.5$ for the FGM law remains rather demanding, see for example the use of $M = 100$ for the second frequency investigated in Table 10 in the case of thin cylinder with $p = 0.5$ and $m = n = 2$.

Table 8. One-layered FGM cylindrical shell with $p = 2.0$ and $R_\alpha/h = 10$. First three modes for $m = n = 2$ given as dimensionless circular frequency $\bar{\omega} = (\omega/10)(R_\alpha/h)^2\sqrt{\rho_c/E_c}$. One physical layer ($N_L = 1$) divided in M mathematical layers.

$p = 2.0$; $m = 2$, $n = 2$; $R_\alpha/h = 10$; I mode

	$N=1$	$N=2$	$N=3$	$N=4$	$N=5$	$N=6$	$N=7$	$N=8$	$N=9$	$N=10$	$N=11$	$N=12$
$M=1$	NaN	1.5993	0.6104	0.9439	0.8869	0.8938	0.8929	0.8930	0.8930	0.8930	0.8930	0.8926
$M=10$	0.8163	0.8194	0.8623	0.8624	0.8624	0.8624	0.8624	0.8624	0.8624	0.8624	0.8624	0.8624
$M=20$	0.8412	0.8652	0.8630	0.8630	0.8630	0.8630	0.8630	0.8630	0.8630	0.8630	0.8630	0.8630
$M=40$	0.8526	0.8637	**0.8632**	**0.8632**	**0.8632**	**0.8632**	**0.8632**	**0.8632**	**0.8632**	**0.8632**	**0.8632**	**0.8632**
$M=60$	0.8562	0.8634	**0.8632**	**0.8632**	**0.8632**	**0.8632**	**0.8632**	**0.8632**	**0.8632**	**0.8632**	**0.8632**	**0.8632**
$M=80$	0.8580	0.8633	**0.8632**	**0.8632**	**0.8632**	**0.8632**	**0.8632**	**0.8632**	**0.8632**	**0.8632**	**0.8632**	**0.8632**
$M=100$	0.8590	0.8633	**0.8632**	**0.8632**	**0.8632**	**0.8632**	**0.8632**	**0.8632**	**0.8632**	**0.8632**	**0.8632**	**0.8632**

$p = 2.0$; $m = 2$, $n = 2$; $R_\alpha/h = 10$; II mode

	$N=1$	$N=2$	$N=3$	$N=4$	$N=5$	$N=6$	$N=7$	$N=8$	$N=9$	$N=10$	$N=11$	$N=12$
$M=1$	NaN	2.9777	2.9665	2.9679	2.9677	2.9677	2.9677	2.9677	2.9677	2.9677	2.9675	2.9700
$M=10$	3.1422	3.5517	3.1421	3.1421	3.1421	3.1421	3.1421	3.1421	3.1421	3.1421	3.1421	3.1421
$M=20$	3.1433	3.1433	3.1433	3.1433	3.1433	3.1433	3.1433	3.1433	3.1433	3.1433	3.1433	3.1433
$M=40$	3.1436	3.1436	**3.1437**	**3.1437**	**3.1437**	**3.1437**	**3.1437**	**3.1437**	**3.1437**	**3.1437**	**3.1437**	**3.1437**
$M=60$	**3.1437**	**3.1437**	**3.1437**	**3.1437**	**3.1437**	**3.1437**	**3.1437**	**3.1437**	**3.1437**	**3.1437**	**3.1437**	**3.1437**
$M=80$	**3.1437**	**3.1437**	**3.1437**	**3.1437**	**3.1437**	**3.1437**	**3.1437**	**3.1437**	**3.1437**	**3.1437**	**3.1437**	**3.1437**
$M=100$	**3.1437**	**3.1437**	**3.1437**	**3.1437**	**3.1437**	**3.1437**	**3.1437**	**3.1437**	**3.1437**	**3.1437**	**3.1437**	**3.1437**

$p = 2.0$; $m = 2$, $n = 2$; $R_\alpha/h = 10$; III mode

	$N=1$	$N=2$	$N=3$	$N=4$	$N=5$	$N=6$	$N=7$	$N=8$	$N=9$	$N=10$	$N=11$	$N=12$
$M=1$	NaN	4.9482	4.9899	4.9947	4.9927	4.9926	4.9927	4.9927	4.9927	4.9927	4.9928	4.9910
$M=10$	5.3269	4.9907	5.3290	5.3290	5.3290	5.3290	5.3290	5.3290	5.3290	5.3290	5.3290	5.3290
$M=20$	5.3296	5.3309	5.3312	5.3312	5.3312	5.3312	5.3312	5.3312	5.3312	5.3312	5.3312	5.3312
$M=40$	5.3308	5.3317	5.3318	5.3318	5.3318	5.3318	5.3318	5.3318	5.3318	5.3318	5.3318	5.3318
$M=60$	5.3312	**5.3319**	**5.3319**	**5.3319**	**5.3319**	**5.3319**	**5.3319**	**5.3319**	**5.3319**	**5.3319**	**5.3319**	**5.3319**
$M=80$	5.3314	**5.3319**	**5.3319**	**5.3319**	**5.3319**	**5.3319**	**5.3319**	**5.3319**	**5.3319**	**5.3319**	**5.3319**	**5.3319**
$M=100$	5.3315	**5.3319**	**5.3319**	**5.3319**	**5.3319**	**5.3319**	**5.3319**	**5.3319**	**5.3319**	**5.3319**	**5.3319**	**5.3319**

Tables 13 to 16 propose the first three frequencies for the sandwich spherical shell (thin $R_\alpha/h = 100$ and thick $R_\alpha/h = 10$ geometry) with FGM core ($p = 1.0$ or $p = 0.5$) in the cases of half-wave numbers $m = n = 1$ and $m = n = 2$. In these benchmarks, the effect of the p coefficient is very important in the convergence of M mathematical layers as demonstrated by Table 16 for $m = n = 2$. In this benchmark,

Table 9. Sandwich cylinder with FGM core ($p = 1.0$) and $R_\alpha/h = 100$. First three modes for $m = 2$ and $n = 1$ given as dimensionless circular frequency $\bar{\omega} = (\omega/10)(R_\alpha/h)^2\sqrt{\rho_c/E_c}$. Three physical layers ($N_L = 3$) divided in M mathematical layers.

$p = 1.0$; $m = 2$, $n = 1$; $R_\alpha/h = 100$; I mode

	$N=1$	$N=2$	$N=3$	$N=4$	$N=5$	$N=6$	$N=7$	$N=8$	$N=9$	$N=10$	$N=11$	$N=12$
$M=3$	5.9485	5.9334	5.9334	5.9334	5.9334	5.9334	5.9334	5.9334	5.9334	5.9334	5.9334	5.9334
$M=10$	5.9378	5.9332	5.9332	5.9332	5.9332	5.9332	5.9332	5.9332	5.9332	5.9332	5.9332	5.9332
$M=20$	5.9356	**5.9333**	**5.9333**	**5.9333**	**5.9333**	**5.9333**	**5.9333**	**5.9333**	**5.9333**	**5.9333**	**5.9333**	**5.9333**
$M=40$	5.9344	**5.9333**	**5.9333**	**5.9333**	**5.9333**	**5.9333**	**5.9333**	**5.9333**	**5.9333**	**5.9333**	**5.9333**	**5.9333**
$M=60$	5.9340	**5.9333**	**5.9333**	**5.9333**	**5.9333**	**5.9333**	**5.9333**	**5.9333**	**5.9333**	**5.9333**	**5.9333**	**5.9333**
$M=80$	5.9334	**5.9333**	**5.9333**	**5.9333**	**5.9333**	**5.9333**	**5.9333**	**5.9333**	**5.9333**	**5.9333**	**5.9333**	**5.9333**
$M=100$	5.9337	**5.9333**	**5.9333**	**5.9333**	**5.9333**	**5.9333**	**5.9333**	**5.9333**	**5.9333**	**5.9333**	**5.9333**	**5.9333**

$p = 1.0$; $m = 2$, $n = 1$; $R_\alpha/h = 100$; II mode

	$N=1$	$N=2$	$N=3$	$N=4$	$N=5$	$N=6$	$N=7$	$N=8$	$N=9$	$N=10$	$N=11$	$N=12$
$M=3$	66.039	**66.041**	**66.041**	**66.041**	**66.041**	**66.041**	**66.041**	**66.041**	**66.041**	**66.041**	**66.041**	**66.041**
$M=10$	**66.041**	**66.041**	**66.041**	**66.041**	**66.041**	**66.041**	**66.041**	**66.041**	**66.041**	**66.041**	**66.041**	**66.041**
$M=20$	**66.041**	**66.041**	**66.041**	**66.041**	**66.041**	**66.041**	**66.041**	**66.041**	**66.041**	**66.041**	**66.041**	**66.041**
$M=40$	**66.041**	**66.041**	**66.041**	**66.041**	**66.041**	**66.041**	**66.041**	**66.041**	**66.041**	**66.041**	**66.041**	**66.041**
$M=60$	**66.041**	**66.041**	**66.041**	**66.041**	**66.041**	**66.041**	**66.041**	**66.041**	**66.041**	**66.041**	**66.041**	**66.041**
$M=80$	**66.041**	**66.041**	**66.041**	**66.041**	**66.041**	**66.041**	**66.041**	**66.041**	**66.041**	**66.041**	**66.041**	**66.041**
$M=100$	**66.041**	**66.041**	**66.041**	**66.041**	**66.041**	**66.041**	**66.041**	**66.041**	**66.041**	**66.041**	**66.041**	**66.041**

$p = 1.0$; $m = 2$, $n = 1$; $R_\alpha/h = 100$; III mode

	$N=1$	$N=2$	$N=3$	$N=4$	$N=5$	$N=6$	$N=7$	$N=8$	$N=9$	$N=10$	$N=11$	$N=12$
$M=3$	143.28	**143.34**	**143.34**	**143.34**	**143.34**	**143.34**	**143.34**	**143.34**	**143.34**	**143.34**	**143.34**	**143.34**
$M=10$	143.32	**143.34**	**143.34**	**143.34**	**143.34**	**143.34**	**143.34**	**143.34**	**143.34**	**143.34**	**143.34**	**143.34**
$M=20$	143.33	**143.34**	**143.34**	**143.34**	**143.34**	**143.34**	**143.34**	**143.34**	**143.34**	**143.34**	**143.34**	**143.34**
$M=40$	143.33	**143.34**	**143.34**	**143.34**	**143.34**	**143.34**	**143.34**	**143.34**	**143.34**	**143.34**	**143.34**	**143.34**
$M=60$	**143.34**	**143.34**	**143.34**	**143.34**	**143.34**	**143.34**	**143.34**	**143.34**	**143.34**	**143.34**	**143.34**	**143.34**
$M=80$	**143.34**	**143.34**	**143.34**	**143.34**	**143.34**	**143.34**	**143.34**	**143.34**	**143.34**	**143.34**	**143.34**	**143.34**
$M=100$	**143.34**	**143.34**	**143.34**	**143.34**	**143.34**	**143.34**	**143.34**	**143.34**	**143.34**	**143.34**	**143.34**	**143.34**

$M = 100$ mathematical layers are mandatory to guarantee the correct values of the first three frequencies. When a big number of mathematical layers are employed, the use of a very small value for the order N of expansion is possible. The M and N values also depend on the vibration mode, Figure 8 proposes the first three vibration modes for the sandwich spherical shell when the thickness ratio is $R_\alpha/h = 10$,

Table 10. Sandwich cylinder with FGM core ($p = 0.5$) and $R_\alpha/h = 100$. First three modes for $m = 2$ and $n = 2$ given as dimensionless circular frequency $\bar{\omega} = (\omega/10)(R_\alpha/h)^2\sqrt{\rho_c/E_c}$. Three physical layers ($N_L = 3$) divided in M mathematical layers.

$p = 0.5$; $m = 2$, $n = 2$; $R_\alpha/h = 100$; I mode

	$N=1$	$N=2$	$N=3$	$N=4$	$N=5$	$N=6$	$N=7$	$N=8$	$N=9$	$N=10$	$N=11$	$N=12$
$M=3$	18.868	18.854	18.854	18.854	18.854	18.854	18.854	18.854	18.854	18.854	18.854	18.854
$M=10$	18.925	18.921	18.921	18.921	18.921	18.921	18.921	18.921	18.921	18.921	18.921	18.921
$M=20$	18.920	18.918	18.918	18.918	18.918	18.918	18.918	18.918	18.918	18.918	18.918	18.918
$M=40$	18.918	**18.917**	**18.817**	**18.917**	**18.917**	**18.917**	**18.917**	**18.917**	**18.917**	**18.917**	**18.917**	**18.917**
$M=60$	18.918	**18.917**	**18.817**	**18.917**	**18.917**	**18.917**	**18.917**	**18.917**	**18.917**	**18.917**	**18.917**	**18.917**
$M=80$	**18.917**	**18.917**	**18.817**	**18.917**	**18.917**	**18.917**	**18.917**	**18.917**	**18.917**	**18.917**	**18.917**	**18.917**
$M=100$	**18.917**	**18.917**	**18.817**	**18.917**	**18.917**	**18.917**	**18.917**	**18.917**	**18.917**	**18.917**	**18.917**	**18.917**

$p = 0.5$; $m = 2$, $n = 2$; $R_\alpha/h = 100$; II mode

	$N=1$	$N=2$	$N=3$	$N=4$	$N=5$	$N=6$	$N=7$	$N=8$	$N=9$	$N=10$	$N=11$	$N=12$
$M=3$	81.495	81.500	81.500	81.500	81.500	81.500	81.500	81.500	81.500	81.500	81.500	81.500
$M=10$	81.796	81.798	81.798	81.798	81.798	81.798	81.798	81.798	81.798	81.798	81.798	81.798
$M=20$	81.785	81.786	81.786	81.786	81.786	81.786	81.786	81.786	81.786	81.786	81.786	81.786
$M=40$	81.781	81.781	81.781	81.781	81.781	81.781	81.781	81.781	81.781	81.781	81.781	81.781
$M=60$	81.780	81.780	81.780	81.780	81.780	81.780	81.780	81.780	81.780	81.780	81.780	81.780
$M=80$	81.779	81.780	81.780	81.780	81.780	81.780	81.780	81.780	81.780	81.780	81.780	81.780
$M=100$	**81.779**	**81.779**	**81.779**	**81.779**	**81.779**	**81.779**	**81.779**	**81.779**	**81.779**	**81.779**	**81.779**	**81.779**

$p = 0.5$; $m = 2$, $n = 2$; $R_\alpha/h = 100$; III mode

	$N=1$	$N=2$	$N=3$	$N=4$	$N=5$	$N=6$	$N=7$	$N=8$	$N=9$	$N=10$	$N=11$	$N=12$
$M=3$	149.75	149.80	149.81	149.81	149.81	149.81	149.81	149.81	149.81	149.81	149.81	149.81
$M=10$	150.34	150.36	150.36	150.36	150.36	150.36	150.36	150.36	150.36	150.36	150.36	150.36
$M=20$	150.32	150.33	150.33	150.33	150.33	150.33	150.33	150.33	150.33	150.33	150.33	150.33
$M=40$	**150.32**	**150.32**	**150.32**	**150.32**	**150.32**	**150.32**	**150.32**	**150.32**	**150.32**	**150.32**	**150.32**	**150.32**
$M=60$	**150.32**	**150.32**	**150.32**	**150.32**	**150.32**	**150.32**	**150.32**	**150.32**	**150.32**	**150.32**	**150.32**	**150.32**
$M=80$	**150.32**	**150.32**	**150.32**	**150.32**	**150.32**	**150.32**	**150.32**	**150.32**	**150.32**	**150.32**	**150.32**	**150.32**
$M=100$	**150.32**	**150.32**	**150.32**	**150.32**	**150.32**	**150.32**	**150.32**	**150.32**	**150.32**	**150.32**	**150.32**	**150.32**

$m = n = 1$ and $p = 1.0$ case is proposed on the left side of the figure, $m = n = 2$ and $p = 0.5$ case is proposed on the right side of the figure.

From the analysis of Tables 1 to 16, the use of $M = 100$ mathematical layers and $N = 3$ order of expansion for the exponential matrix is highly recommended to obtain correct frequencies for different geometries, materials, lamination

Table 11. Sandwich cylinder with FGM core ($p = 1.0$) and $R_\alpha/h = 10$. First three modes for $m = 2$ and $n = 1$ given as dimensionless circular frequency $\bar{\omega} = (\omega/10)(R_\alpha/h)^2\sqrt{\rho_c/E_c}$. Three physical layers ($N_L = 3$) divided in M mathematical layers.

$p = 1.0$; $m = 2$, $n = 1$; $R_\alpha/h = 10$; I mode

	$N=1$	$N=2$	$N=3$	$N=4$	$N=5$	$N=6$	$N=7$	$N=8$	$N=9$	$N=10$	$N=11$	$N=12$
$M=3$	0.0613	0.0600	0.0599	0.0399	54.667	0.0000	0.0000	0.0000	**0.0599**	**0.0599**	**0.0599**	**0.0599**
$M=10$	0.0635	0.0000	**0.0599**	**0.0599**	**0.0599**	**0.0599**	**0.0599**	**0.0599**	**0.0599**	**0.0599**	**0.0599**	**0.0599**
$M=20$	2.3126	**0.0599**	**0.0599**	**0.0599**	**0.0599**	**0.0599**	**0.0599**	**0.0599**	**0.0599**	**0.0599**	**0.0599**	**0.0599**
$M=40$	0.0600	**0.0599**	**0.0599**	**0.0599**	**0.0599**	**0.0599**	**0.0599**	**0.0599**	**0.0599**	**0.0599**	**0.0599**	**0.0599**
$M=60$	0.0600	**0.0599**	**0.0599**	**0.0599**	**0.0599**	**0.0599**	**0.0599**	**0.0599**	**0.0599**	**0.0599**	**0.0599**	**0.0599**
$M=80$	0.0600	**0.0599**	**0.0599**	**0.0599**	**0.0599**	**0.0599**	**0.0599**	**0.0599**	**0.0599**	**0.0599**	**0.0599**	**0.0599**
$M=100$	**0.0599**	**0.0599**	**0.0599**	**0.0599**	**0.0599**	**0.0599**	**0.0599**	**0.0599**	**0.0599**	**0.0599**	**0.0599**	**0.0599**

$p = 1.0$; $m = 2$, $n = 1$; $R_\alpha/h = 10$; II mode

	$N=1$	$N=2$	$N=3$	$N=4$	$N=5$	$N=6$	$N=7$	$N=8$	$N=9$	$N=10$	$N=11$	$N=12$
$M=3$	0.6562	0.6564	0.6564	18.967	58.213	53.385	53.385	53.385	**0.6564**	**0.6564**	**0.6564**	**0.6564**
$M=10$	0.6564	52.342	0.6565	0.6565	0.6565	0.6565	0.6565	0.6565	0.6565	0.6565	0.6565	0.6565
$M=20$	18.957	**0.6564**	**0.6564**	**0.6564**	**0.6564**	**0.6564**	**0.6564**	**0.6564**	**0.6564**	**0.6564**	**0.6564**	**0.6564**
$M=40$	**0.6564**	**0.6564**	**0.6564**	**0.6564**	**0.6564**	**0.6564**	**0.6564**	**0.6564**	**0.6564**	**0.6564**	**0.6564**	**0.6564**
$M=60$	**0.6564**	**0.6564**	**0.6564**	**0.6564**	**0.6564**	**0.6564**	**0.6564**	**0.6564**	**0.6564**	**0.6564**	**0.6564**	**0.6564**
$M=80$	**0.6564**	**0.6564**	**0.6564**	**0.6564**	**0.6564**	**0.6564**	**0.6564**	**0.6564**	**0.6564**	**0.6564**	**0.6564**	**0.6564**
$M=100$	**0.6564**	**0.6564**	**0.6564**	**0.6564**	**0.6564**	**0.6564**	**0.6564**	**0.6564**	**0.6564**	**0.6564**	**0.6564**	**0.6564**

$p = 1.0$; $m = 2$, $n = 1$; $R_\alpha/h = 10$; III mode

	$N=1$	$N=2$	$N=3$	$N=4$	$N=5$	$N=6$	$N=7$	$N=8$	$N=9$	$N=10$	$N=11$	$N=12$
$M=3$	1.4165	1.4225	1.4227	19.025	71.801	73.957	75.499	75.499	**1.4227**	**1.4227**	**1.4227**	**1.4227**
$M=10$	1.4209	65.999	**1.4227**	**1.4227**	**1.4227**	**1.4227**	**1.4227**	**1.4227**	**1.4227**	**1.4227**	**1.4227**	**1.4227**
$M=20$	19.326	**1.4227**	**1.4227**	**1.4227**	**1.4227**	**1.4227**	**1.4227**	**1.4227**	**1.4227**	**1.4227**	**1.4227**	**1.4227**
$M=40$	1.4222	**1.4227**	**1.4227**	**1.4227**	**1.4227**	**1.4227**	**1.4227**	**1.4227**	**1.4227**	**1.4227**	**1.4227**	**1.4227**
$M=60$	1.4224	**1.4227**	**1.4227**	**1.4227**	**1.4227**	**1.4227**	**1.4227**	**1.4227**	**1.4227**	**1.4227**	**1.4227**	**1.4227**
$M=80$	1.4224	**1.4227**	**1.4227**	**1.4227**	**1.4227**	**1.4227**	**1.4227**	**1.4227**	**1.4227**	**1.4227**	**1.4227**	**1.4227**
$M=100$	1.4225	**1.4227**	**1.4227**	**1.4227**	**1.4227**	**1.4227**	**1.4227**	**1.4227**	**1.4227**	**1.4227**	**1.4227**	**1.4227**

sequences, FGM laws, half-wave numbers, frequency orders, and vibration modes. This choice is also confirmed by the comparison of the present 3D model ($M = 100$ and $N = 3$) with other 3D models proposed in the literature. The first assessment proposed by Li et al. [29] considers a simply supported square sandwich plate. The sandwich plate has two external skins with thickness $h_1 = h_3 = 0.1\,h$ and an internal

Table 12. Sandwich cylinder with FGM core ($p = 0.5$) and $R_\alpha/h = 10$. First three modes for $m = 2$ and $n = 2$ given as dimensionless circular frequency $\bar{\omega} = (\omega/10)(R_\alpha/h)^2\sqrt{\rho_c/E_c}$. Three physical layers ($N_L = 3$) divided in M mathematical layers.

$p = 0.5$; $m = 2$, $n = 2$; $R_\alpha/h = 10$; I mode

	$N=1$	$N=2$	$N=3$	$N=4$	$N=5$	$N=6$	$N=7$	$N=8$	$N=9$	$N=10$	$N=11$	$N=12$
$M=3$	0.1912	0.1899	0.1899	0.2111	NaN	0.0000	0.0000	0.0000	0.1899	0.1899	0.1899	0.1899
$M=10$	0.1908	0.0003	**0.1904**	**0.1904**	**0.1904**	**0.1904**	**0.1904**	**0.1904**	**0.1904**	**0.1904**	**0.1904**	**0.1904**
$M=20$	0.0901	**0.1904**	**0.1904**	**0.1904**	**0.1904**	**0.1904**	**0.1904**	**0.1904**	**0.1904**	**0.1904**	**0.1904**	**0.1904**
$M=40$	0.1905	**0.1904**	**0.1904**	**0.1904**	**0.1904**	**0.1904**	**0.1904**	**0.1904**	**0.1904**	**0.1904**	**0.1904**	**0.1904**
$M=60$	0.1905	**0.1904**	**0.1904**	**0.1904**	**0.1904**	**0.1904**	**0.1904**	**0.1904**	**0.1904**	**0.1904**	**0.1904**	**0.1904**
$M=80$	**0.1904**	**0.1904**	**0.1904**	**0.1904**	**0.1904**	**0.1904**	**0.1904**	**0.1904**	**0.1904**	**0.1904**	**0.1904**	**0.1904**
$M=100$	**0.1904**	**0.1904**	**0.1904**	**0.1904**	**0.1904**	**0.1904**	**0.1904**	**0.1904**	**0.1904**	**0.1904**	**0.1904**	**0.1904**

$p = 0.5$; $m = 2$, $n = 2$; $R_\alpha/h = 10$; II mode

	$N=1$	$N=2$	$N=3$	$N=4$	$N=5$	$N=6$	$N=7$	$N=8$	$N=9$	$N=10$	$N=11$	$N=12$
$M=3$	0.8110	0.8117	0.8116	0.7056	NaN	53.385	53.385	53.385	0.8116	0.8116	0.8116	0.8116
$M=10$	0.8147	51.438	0.8149	0.8149	0.8149	0.8149	0.8149	0.8149	0.8149	0.8149	0.8149	0.8149
$M=20$	37.574	0.8148	0.8148	0.8148	0.8148	0.8148	0.8148	0.8148	0.8148	0.8148	0.8148	0.8148
$M=40$	**0.8147**	**0.8147**	**0.8147**	**0.8147**	**0.8147**	**0.8147**	**0.8147**	**0.8147**	**0.8147**	**0.8147**	**0.8147**	**0.8147**
$M=60$	**0.8147**	**0.8147**	**0.8147**	**0.8147**	**0.8147**	**0.8147**	**0.8147**	**0.8147**	**0.8147**	**0.8147**	**0.8147**	**0.8147**
$M=80$	**0.8147**	**0.8147**	**0.8147**	**0.8147**	**0.8147**	**0.8147**	**0.8147**	**0.8147**	**0.8147**	**0.8147**	**0.8147**	**0.8147**
$M=100$	**0.8147**	**0.8147**	**0.8147**	**0.8147**	**0.8147**	**0.8147**	**0.8147**	**0.8147**	**0.8147**	**0.8147**	**0.8147**	**0.8147**

$p = 0.5$; $m = 2$, $n = 2$; $R_\alpha/h = 10$; III mode

	$N=1$	$N=2$	$N=3$	$N=4$	$N=5$	$N=6$	$N=7$	$N=8$	$N=9$	$N=10$	$N=11$	$N=12$
$M=3$	1.4828	1.4885	1.4886	1.5397	NaN	73.251	75.498	75.498	1.4886	1.4886	1.4886	1.4886
$M=10$	1.4929	67.853	1.4947	1.4947	1.4947	1.4947	1.4947	1.4947	1.4947	1.4947	1.4947	1.4947
$M=20$	38.283	1.4944	1.4944	1.4944	1.4944	1.4944	1.4944	1.4944	1.4944	1.4944	1.4944	1.4944
$M=40$	1.4939	**1.4943**	**1.4943**	**1.4943**	**1.4943**	**1.4943**	**1.4943**	**1.4943**	**1.4943**	**1.4943**	**1.4943**	**1.4943**
$M=60$	1.4940	**1.4943**	**1.4943**	**1.4943**	**1.4943**	**1.4943**	**1.4943**	**1.4943**	**1.4943**	**1.4943**	**1.4943**	**1.4943**
$M=80$	1.4940	**1.4943**	**1.4943**	**1.4943**	**1.4943**	**1.4943**	**1.4943**	**1.4943**	**1.4943**	**1.4943**	**1.4943**	**1.4943**
$M=100$	1.4941	**1.4943**	**1.4943**	**1.4943**	**1.4943**	**1.4943**	**1.4943**	**1.4943**	**1.4943**	**1.4943**	**1.4943**	**1.4943**

core with thickness $h_2 = 0.8\,h$. The bottom skin is full ceramic and the top skin is full metallic, the core is in FGM. The metallic (m) material has Young's modulus $E_m = 70\,\text{GPa}$, mass density $\rho_m = 2707\,\text{kg/m}^3$ and Poisson's ratio $\nu_m = 0.3$. The ceramic (c) material has Young's modulus $E_c = 380\,\text{GPa}$, mass density $\rho_c = 3800\,\text{kg/m}^3$, and Poisson's ratio $\nu_c = 0.3$. The functionally graded core has constant Poisson's ratio $\nu = 0.3$. Young's modulus and mass density continuously vary

Table 13. Sandwich spherical shell with FGM core ($p = 1.0$) and $R_\alpha/h = 100$. First three modes for $m = n = 1$ given as dimensionless circular frequency $\bar{\omega} = (\omega/10)(R_\alpha/h)^2\sqrt{\rho_c/E_c}$. Three physical layers ($N_L = 3$) divided in M mathematical layers.

$p = 1.0$; $m = 1$, $n = 1$; $R_\alpha/h = 100$; I mode

	$N=1$	$N=2$	$N=3$	$N=4$	$N=5$	$N=6$	$N=7$	$N=8$	$N=9$	$N=10$	$N=11$	$N=12$
$M=3$	90.206	91.305	**91.277**	**91.277**	**91.277**	**91.277**	**91.277**	**91.277**	**91.277**	**91.277**	**91.277**	**91.277**
$M=10$	90.961	91.281	91.278	91.278	91.278	91.278	91.278	91.278	91.278	91.278	91.278	91.278
$M=20$	91.119	91.278	**91.277**	**91.277**	**91.277**	**91.277**	**91.277**	**91.277**	**91.277**	**91.277**	**91.277**	**91.277**
$M=40$	91.198	**91.277**	**91.277**	**91.277**	**91.277**	**91.277**	**91.277**	**91.277**	**91.277**	**91.277**	**91.277**	**91.277**
$M=60$	91.225	**91.277**	**91.277**	**91.277**	**91.277**	**91.277**	**91.277**	**91.277**	**91.277**	**91.277**	**91.277**	**91.277**
$M=80$	91.238	**91.277**	**91.277**	**91.277**	**91.277**	**91.277**	**91.277**	**91.277**	**91.277**	**91.277**	**91.277**	**91.277**
$M=100$	91.246	**91.277**	**91.277**	**91.277**	**91.277**	**91.277**	**91.277**	**91.277**	**91.277**	**91.277**	**91.277**	**91.277**

$p = 1.0$; $m = 1$, $n = 1$; $R_\alpha/h = 100$; II mode

	$N=1$	$N=2$	$N=3$	$N=4$	$N=5$	$N=6$	$N=7$	$N=8$	$N=9$	$N=10$	$N=11$	$N=12$
$M=3$	251.59	**251.61**	**251.61**	**251.61**	**251.61**	**251.61**	**251.61**	**251.61**	**251.61**	**251.61**	**251.61**	**251.61**
$M=10$	251.60	**251.61**	**251.61**	**251.61**	**251.61**	**251.61**	**251.61**	**251.61**	**251.61**	**251.61**	**251.61**	**251.61**
$M=20$	**251.61**	**251.61**	**251.61**	**251.61**	**251.61**	**251.61**	**251.61**	**251.61**	**251.61**	**251.61**	**251.61**	**251.61**
$M=40$	**251.61**	**251.61**	**251.61**	**251.61**	**251.61**	**251.61**	**251.61**	**251.61**	**251.61**	**251.61**	**251.61**	**251.61**
$M=60$	**251.61**	**251.61**	**251.61**	**251.61**	**251.61**	**251.61**	**251.61**	**251.61**	**251.61**	**251.61**	**251.61**	**251.61**
$M=80$	**251.61**	**251.61**	**251.61**	**251.61**	**251.61**	**251.61**	**251.61**	**251.61**	**251.61**	**251.61**	**251.61**	**251.61**
$M=100$	**251.61**	**251.61**	**251.61**	**251.61**	**251.61**	**251.61**	**251.61**	**251.61**	**251.61**	**251.61**	**251.61**	**251.61**

$p = 1.0$; $m = 1$, $n = 1$; $R_\alpha/h = 100$; III mode

	$N=1$	$N=2$	$N=3$	$N=4$	$N=5$	$N=6$	$N=7$	$N=8$	$N=9$	$N=10$	$N=11$	$N=12$
$M=3$	445.61	445.78	**445.79**	**445.79**	**445.79**	**445.79**	**445.79**	**445.79**	**445.79**	**445.79**	**445.79**	**445.79**
$M=10$	445.73	**445.79**	**445.79**	**445.79**	**445.79**	**445.79**	**445.79**	**445.79**	**445.79**	**445.79**	**445.79**	**445.79**
$M=20$	445.76	**445.79**	**445.79**	**445.79**	**445.79**	**445.79**	**445.79**	**445.79**	**445.79**	**445.79**	**445.79**	**445.79**
$M=40$	445.77	**445.79**	**445.79**	**445.79**	**445.79**	**445.79**	**445.79**	**445.79**	**445.79**	**445.79**	**445.79**	**445.79**
$M=60$	445.78	**445.79**	**445.79**	**445.79**	**445.79**	**445.79**	**445.79**	**445.79**	**445.79**	**445.79**	**445.79**	**445.79**
$M=80$	445.78	**445.79**	**445.79**	**445.79**	**445.79**	**445.79**	**445.79**	**445.79**	**445.79**	**445.79**	**445.79**	**445.79**
$M=100$	445.78	**445.79**	**445.79**	**445.79**	**445.79**	**445.79**	**445.79**	**445.79**	**445.79**	**445.79**	**445.79**	**445.79**

through the thickness direction z as proposed in equations (35) and (36) where the volume fraction of ceramic phase is replaced by the volume fraction of metallic phase in accordance with the following equation

$$V_m = 1 - V_c = 1 - (0.5 + z/0.8h)^p \tag{38}$$

Table 14. Sandwich spherical shell with FGM core ($p = 0.5$) and $R_\alpha/h = 100$. First three modes for $m = n = 2$ given as dimensionless circular frequency $\bar{\omega} = (\omega/10)(R_\alpha/h)^2\sqrt{\rho_c/E_c}$. Three physical layers ($N_L = 3$) divided in M mathematical layers.

$p = 0.5$; $m = 2$, $n = 2$; $R_\alpha/h = 100$; I mode

	$N=1$	$N=2$	$N=3$	$N=4$	$N=5$	$N=6$	$N=7$	$N=8$	$N=9$	$N=10$	$N=11$	$N=12$
$M=3$	91.480	97.467	96.977	96.979	96.979	96.979	96.979	96.979	96.979	96.979	96.979	96.979
$M=10$	95.795	97.408	97.365	97.365	97.365	97.365	97.365	97.365	97.365	97.365	97.365	97.365
$M=20$	96.569	97.356	97.345	97.345	97.345	97.345	97.345	97.345	97.345	97.345	97.345	97.345
$M=40$	96.952	97.341	97.338	97.338	97.338	97.338	97.338	97.338	97.338	97.338	97.338	97.338
$M=60$	97.079	97.337	97.336	97.336	97.336	97.336	97.336	97.336	97.336	97.336	97.336	97.336
$M=80$	97.143	97.336	**97.335**	**97.335**	**97.335**	**97.335**	**97.335**	**97.335**	**97.335**	**97.335**	**97.335**	**97.335**
$M=100$	97.181	**97.335**	**97.335**	**97.335**	**97.335**	**97.335**	**97.335**	**97.335**	**97.335**	**97.335**	**97.335**	**97.335**

$p = 0.5$; $m = 2$, $n = 2$; $R_\alpha/h = 100$; II mode

	$N=1$	$N=2$	$N=3$	$N=4$	$N=5$	$N=6$	$N=7$	$N=8$	$N=9$	$N=10$	$N=11$	$N=12$
$M=3$	507.31	507.32	507.32	507.32	507.32	507.32	507.32	507.32	507.32	507.32	507.32	507.32
$M=10$	509.16	509.16	509.16	509.16	509.16	509.16	509.16	509.16	509.16	509.16	509.16	509.16
$M=20$	509.09	509.09	509.09	509.09	509.09	509.09	509.09	509.09	509.09	509.09	509.09	509.09
$M=40$	509.06	509.06	509.06	509.06	509.06	509.06	509.06	509.06	509.06	509.06	509.06	509.06
$M=60$	**509.05**	**509.05**	**509.05**	**509.05**	**509.05**	**509.05**	**509.05**	**509.05**	**509.05**	**509.05**	**509.05**	**509.05**
$M=80$	**509.05**	**509.05**	**509.05**	**509.05**	**509.05**	**509.05**	**509.05**	**509.05**	**509.05**	**509.05**	**509.05**	**509.05**
$M=100$	**509.05**	**509.05**	**509.05**	**509.05**	**509.05**	**509.05**	**509.05**	**509.05**	**509.05**	**509.05**	**509.05**	**509.05**

$p = 0.5$; $m = 2$, $n = 2$; $R_\alpha/h = 100$; III mode

	$N=1$	$N=2$	$N=3$	$N=4$	$N=5$	$N=6$	$N=7$	$N=8$	$N=9$	$N=10$	$N=11$	$N=12$
$M=3$	867.46	867.73	867.75	867.75	867.75	867.75	867.75	867.75	867.75	867.75	867.75	867.75
$M=10$	870.80	870.88	870.88	870.88	870.88	870.88	870.88	870.88	870.88	870.88	870.88	870.88
$M=20$	870.71	870.76	870.76	870.76	870.76	870.76	870.76	870.76	870.76	870.76	870.76	870.76
$M=40$	870.69	870.71	870.71	870.71	870.71	870.71	870.71	870.71	870.71	870.71	870.71	870.71
$M=60$	870.68	870.70	870.70	870.70	870.70	870.70	870.70	870.70	870.70	870.70	870.70	870.70
$M=80$	870.68	**870.69**	**870.69**	**870.69**	**870.69**	**870.69**	**870.69**	**870.69**	**870.69**	**870.69**	**870.69**	**870.69**
$M=100$	870.68	**870.69**	**870.69**	**870.69**	**870.69**	**870.69**	**870.69**	**870.69**	**870.69**	**870.69**	**870.69**	**870.69**

V_c and V_m are the volume fraction of ceramic phase and metallic phase, respectively. z varies from $-0.8h/2$ to $0.8h/2$. The second assessment by Zahedinejad et al. [38] considers a simply supported cylindrical shell panel. The shell has the two dimensions a and b that are coincident ($a = b$), the investigated thickness ratio is a/h equals 5. Two different radii of curvature R_α are considered, which means a/R_α equals 0.5 or 1. The radius of curvature R_β is infinite. The shell is one-layered and it

Table 15. Sandwich spherical shell with FGM core ($p = 1.0$) and $R_\alpha/h = 10$. First three modes for $m = n = 1$ given as dimensionless circular frequency $\bar{\omega} = (\omega/10)(R_\alpha/h)^2\sqrt{\rho_c/E_c}$. Three physical layers ($N_L = 3$) divided in M mathematical layers.

$p = 1.0$; $m = 1$, $n = 1$; $R_\alpha/h = 10$; I mode

	$N=1$	$N=2$	$N=3$	$N=4$	$N=5$	$N=6$	$N=7$	$N=8$	$N=9$	$N=10$	$N=11$	$N=12$
$M=3$	0.8846	1.0119	0.9851	0.9837	54.161	NaN	53.385	0.0000	0.9864	0.9864	0.9864	0.9864
$M=10$	0.9593	62.414	0.9863	0.9863	0.9863	0.9863	0.9863	0.9863	0.9863	0.9863	0.9863	0.9863
$M=20$	1.0756	0.9866	0.9861	0.9861	0.9861	0.9861	0.9861	0.9861	0.9861	0.9861	0.9861	0.9861
$M=40$	0.9795	0.9861	**0.9860**	**0.9860**	**0.9860**	**0.9860**	**0.9860**	**0.9860**	**0.9860**	**0.9860**	**0.9860**	**0.9860**
$M=60$	0.9817	0.9861	**0.9860**	**0.9860**	**0.9860**	**0.9860**	**0.9860**	**0.9860**	**0.9860**	**0.9860**	**0.9860**	**0.9860**
$M=80$	0.9828	**0.9860**	**0.9860**	**0.9860**	**0.9860**	**0.9860**	**0.9860**	**0.9860**	**0.9860**	**0.9860**	**0.9860**	**0.9860**
$M=100$	0.9834	**0.9860**	**0.9860**	**0.9860**	**0.9860**	**0.9860**	**0.9860**	**0.9860**	**0.9860**	**0.9860**	**0.9860**	**0.9860**

$p = 1.0$; $m = 1$, $n = 1$; $R_\alpha/h = 10$; II mode

	$N=1$	$N=2$	$N=3$	$N=4$	$N=5$	$N=6$	$N=7$	$N=8$	$N=9$	$N=10$	$N=11$	$N=12$
$M=3$	2.4988	2.5010	2.5010	2.5113	58.173	NaN	75.498	53.385	2.5010	2.5010	2.5010	2.5010
$M=10$	2.5000	96.643	2.5006	2.5006	2.5006	2.5006	2.5006	2.5006	2.5006	2.5006	2.5006	2.5006
$M=20$	2.1846	**2.5005**	**2.5005**	**2.5005**	**2.5005**	**2.5005**	**2.5005**	**2.5005**	**2.5005**	**2.5005**	**2.5005**	**2.5005**
$M=40$	2.5004	**2.5005**	**2.5005**	**2.5005**	**2.5005**	**2.5005**	**2.5005**	**2.5005**	**2.5005**	**2.5005**	**2.5005**	**2.5005**
$M=60$	2.5004	**2.5005**	**2.5005**	**2.5005**	**2.5005**	**2.5005**	**2.5005**	**2.5005**	**2.5005**	**2.5005**	**2.5005**	**2.5005**
$M=80$	2.5004	**2.5005**	**2.5005**	**2.5005**	**2.5005**	**2.5005**	**2.5005**	**2.5005**	**2.5005**	**2.5005**	**2.5005**	**2.5005**
$M=100$	2.5004	**2.5005**	**2.5005**	**2.5005**	**2.5005**	**2.5005**	**2.5005**	**2.5005**	**2.5005**	**2.5005**	**2.5005**	**2.5005**

$p = 1.0$; $m = 1$, $n = 1$; $R_\alpha/h = 10$; III mode

	$N=1$	$N=2$	$N=3$	$N=4$	$N=5$	$N=6$	$N=7$	$N=8$	$N=9$	$N=10$	$N=11$	$N=12$
$M=3$	4.4065	4.4211	4.4235	4.4175	60.567	NaN	92.731	75.499	4.4234	4.4234	4.4234	4.4234
$M=10$	4.4169	98.974	4.4223	4.4223	4.4223	4.4223	4.4223	4.4223	4.4223	4.4223	4.4223	4.4223
$M=20$	4.5765	**4.4221**	**4.4221**	**4.4221**	**4.4221**	**4.4221**	**4.4221**	**4.4221**	**4.4221**	**4.4221**	**4.4221**	**4.4221**
$M=40$	4.4207	**4.4221**	**4.4221**	**4.4221**	**4.4221**	**4.4221**	**4.4221**	**4.4221**	**4.4221**	**4.4221**	**4.4221**	**4.4221**
$M=60$	4.4212	**4.4221**	**4.4221**	**4.4221**	**4.4221**	**4.4221**	**4.4221**	**4.4221**	**4.4221**	**4.4221**	**4.4221**	**4.4221**
$M=80$	4.4214	**4.4221**	**4.4221**	**4.4221**	**4.4221**	**4.4221**	**4.4221**	**4.4221**	**4.4221**	**4.4221**	**4.4221**	**4.4221**
$M=100$	4.4215	**4.4221**	**4.4221**	**4.4221**	**4.4221**	**4.4221**	**4.4221**	**4.4221**	**4.4221**	**4.4221**	**4.4221**	**4.4221**

is made of a functionally graded material. In this case, the structure is fully metallic at the bottom and fully ceramic at the top. This feature means that equations (35) to (37) are still valid. The metallic phase and the ceramic phase have the properties already seen for the first assessment by Li et al. [29]. The only difference is for ρ_m, which is equal to $2702\,\mathrm{kg/m^3}$ (the first assessment considers $\rho_m = 2707\,\mathrm{kg/m^3}$). Table 17 shows the comparison with the 3D model by Li et al. [29] for a sandwich

Table 16. Sandwich spherical shell with FGM core ($p = 0.5$) and $R_\alpha/h = 10$. First three modes for $m = n = 2$ given as dimensionless circular frequency $\bar{\omega} = (\omega/10)(R_\alpha/h)^2\sqrt{\rho_c/E_c}$. Three physical layers ($N_L = 3$) divided in M mathematical layers.

$p = 0.5$; $m = 2$, $n = 2$; $R_\alpha/h = 10$; I mode

	$N=1$	$N=2$	$N=3$	$N=4$	$N=5$	$N=6$	$N=7$	$N=8$	$N=9$	$N=10$	$N=11$	$N=12$
$M=3$	1.6476	2.0859	1.8905	1.9068	53.370	NaN	53.385	0.0000	1.9046	1.9046	1.9046	1.9046
$M=10$	1.8665	0.0335	1.9255	1.9258	1.9258	1.9258	1.9258	1.9258	1.9258	1.9258	1.9258	1.9258
$M=20$	1.9041	1.9273	1.9237	1.9237	1.9237	1.9237	1.9237	1.9237	1.9237	1.9237	1.9237	1.9237
$M=40$	1.9093	1.9239	1.9230	1.9230	1.9230	1.9230	1.9230	1.9230	1.9230	1.9230	1.9230	1.9230
$M=60$	1.9138	1.9233	1.9229	1.9229	1.9229	1.9229	1.9229	1.9229	1.9229	1.9229	1.9229	1.9229
$M=80$	1.9160	1.9230	**1.9228**	**1.9228**	**1.9228**	**1.9228**	**1.9228**	**1.9228**	**1.9228**	**1.9228**	**1.9228**	**1.9228**
$M=100$	1.9173	1.9229	**1.9228**	**1.9228**	**1.9228**	**1.9228**	**1.9228**	**1.9228**	**1.9228**	**1.9228**	**1.9228**	**1.9228**

$p = 0.5$; $m = 2$, $n = 2$; $R_\alpha/h = 10$; II mode

	$N=1$	$N=2$	$N=3$	$N=4$	$N=5$	$N=6$	$N=7$	$N=8$	$N=9$	$N=10$	$N=11$	$N=12$
$M=3$	5.0424	5.0428	5.0430	5.0408	61.530	NaN	75.498	53.385	5.0430	5.0430	5.0430	5.0430
$M=10$	5.0619	52.748	5.0622	5.0622	5.0622	5.0622	5.0622	5.0622	5.0622	5.0622	5.0622	5.0622
$M=20$	5.0229	5.0612	5.0612	5.0612	5.0612	5.0612	5.0612	5.0612	5.0612	5.0612	5.0612	5.0612
$M=40$	5.0608	5.0609	5.0609	5.0609	5.0609	5.0609	5.0609	5.0609	5.0609	5.0609	5.0609	5.0609
$M=60$	5.0607	5.0608	5.0608	5.0608	5.0608	5.0608	5.0608	5.0608	5.0608	5.0608	5.0608	5.0608
$M=80$	5.0607	5.0608	5.0608	5.0608	5.0608	5.0608	5.0608	5.0608	5.0608	5.0608	5.0608	5.0608
$M=100$	**5.0607**	**5.0607**	**5.0607**	**5.0607**	**5.0607**	**5.0607**	**5.0607**	**5.0607**	**5.0607**	**5.0607**	**5.0607**	**5.0607**

$p = 0.5$; $m = 2$, $n = 2$; $R_\alpha/h = 10$; III mode

	$N=1$	$N=2$	$N=3$	$N=4$	$N=5$	$N=6$	$N=7$	$N=8$	$N=9$	$N=10$	$N=11$	$N=12$
$M=3$	8.5594	8.5676	8.5836	8.5851	67.175	NaN	92.555	75.497	8.5831	8.5831	8.5831	8.5831
$M=10$	8.6030	66.595	8.6124	8.6124	8.6124	8.6124	8.6124	8.6124	8.6124	8.6124	8.6124	8.6124
$M=20$	8.6344	8.6106	8.6109	8.6109	8.6109	8.6109	8.6109	8.6109	8.6109	8.6109	8.6109	8.6109
$M=40$	8.6079	8.6103	8.6104	8.6104	8.6104	8.6104	8.6104	8.6104	8.6104	8.6104	8.6104	8.6104
$M=60$	8.6086	8.6102	8.6103	8.6103	8.6103	8.6103	8.6103	8.6103	8.6103	8.6103	8.6103	8.6103
$M=80$	8.6090	**8.6102**	**8.6102**	**8.6102**	**8.6102**	**8.6102**	**8.6102**	**8.6102**	**8.6102**	**8.6102**	**8.6102**	**8.6102**
$M=100$	8.6092	**8.6102**	**8.6102**	**8.6102**	**8.6102**	**8.6102**	**8.6102**	**8.6102**	**8.6102**	**8.6102**	**8.6102**	**8.6102**

plate with FGM core, and several p values and thickness ratios a/h are considered for the first fundamental circular frequency $\bar{\omega} = \omega\frac{a^2}{h}\sqrt{\frac{\rho_0}{E_0}}$ (with $E_0 = 1\,\text{GPa}$ and $\rho_0 = 1\,\text{kg/m}^3$) in the case of half-wave numbers $m = n = 1$. Small differences are due to the fact the present model is an exact closed form 3D model while Li et al. [29] proposed a 3D model numerically solved by means of the Ritz approach. Table 18 shows the comparison of the present 3D exact model with the 3D solution

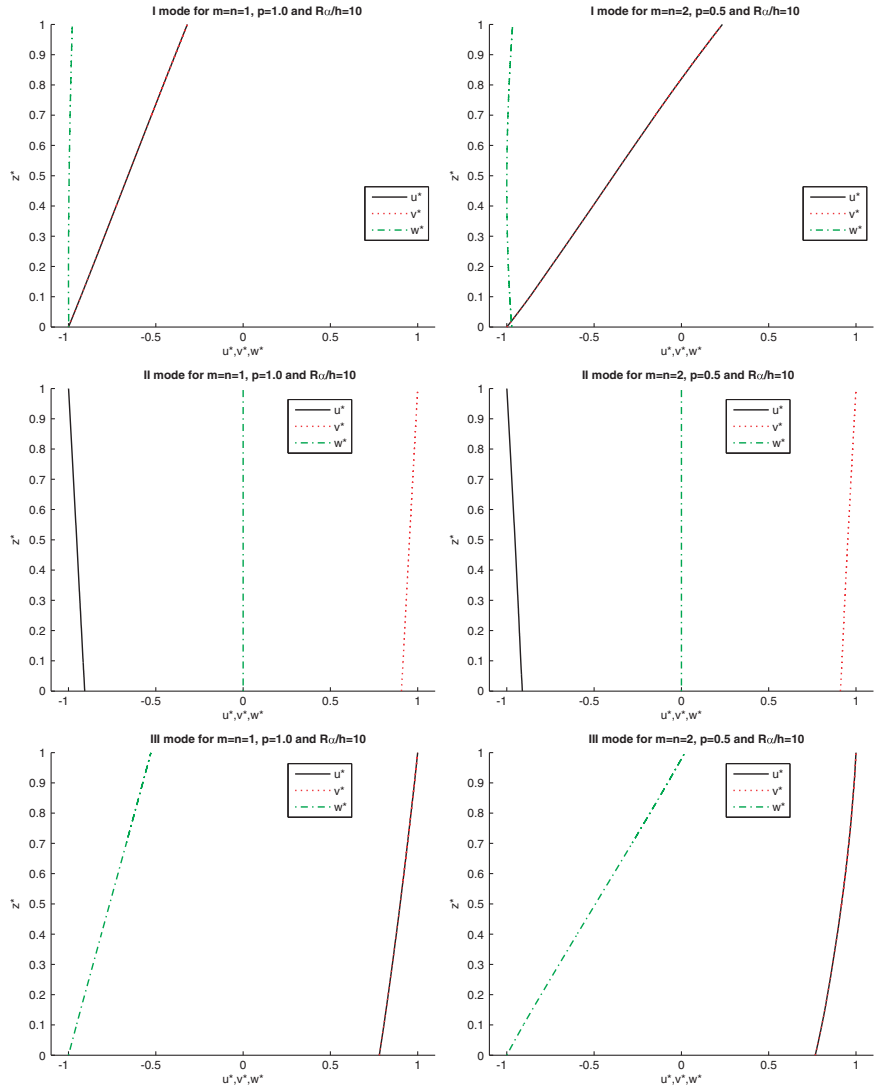

Figure 8. First three vibration modes for sandwich spherical shell panel ($R_\alpha/h = 10$) with FGM ($p = 1.0$ and 0.5) core and $m = n = 1$ and $m = n = 2$.

by Zahedinejad et al. [38] for a thick one-layered FGM cylindrical shell panel. For imposed half-wave numbers $m = n = 1$, the fundamental circular frequencies $\bar{\omega} = \omega h \sqrt{\frac{\rho_c}{E_c}}$ are compared for several p parameters and two different in-plane dimension/curvature ratios a/R_α. The two solutions are very closed, and the

Table 17. Sandwich plate with FGM core. Fundamental circular frequency $\bar{\omega} = \omega \frac{a^2}{h}\sqrt{\frac{\rho_0}{E_0}}$ for half-wave numbers $m = n = 1$ and different thickness ratios a/h and exponents p for the material law. Comparison between the 3D model based on Ritz approach by Li et al. [29] and the present 3D exact solution ($M = 100$, $N = 3$).

p	0.5	1.0	2.0	5.0	10
	$a/h = 5$				
Present 3D	1.19575	1.25337	1.31566	1.39564	1.44537
Li et al. [29]	1.19580	1.25338	1.31569	1.39567	1.44540
	$a/h = 10$				
Present 3D	1.29748	1.34848	1.40829	1.49311	1.54984
Li et al. [29]	1.29751	1.34847	1.40828	1.49309	1.54980
	$a/h = 100$				
Present 3D	1.33928	1.38671	1.44494	1.53148	1.59113
Li et al. [29]	1.33931	1.38669	1.44491	1.53143	1.59105

Table 18. One-layered FGM cylindrical shell panel with thickness ratio $a/h = 5$. Fundamental circular frequency $\bar{\omega} = \omega h\sqrt{\frac{\rho_c}{E_c}}$ for half-wave numbers $m = n = 1$ and different radii of curvature R_α and exponents p for the material law. Comparison between the 3D model based on the differential quadrature method by Zahedinejad et al. [38] and the present 3D exact solution ($M = 100$, $N = 3$).

p	0.0	0.5	1.0	4.0	10
	$a/R_\alpha = 1.0$				
Present 3D	0.2155	0.1848	0.1671	0.1392	0.1300
Zahedinejad et al. [38]	0.2164	0.1852	0.1676	0.1394	0.1286
	$a/R_\alpha = 0.5$				
Present 3D	0.2129	0.1817	0.1638	0.1374	0.1296
Zahedinejad et al. [38]	0.2113	0.1814	0.1639	0.1367	0.1271

small differences are due to the fact that the 3D model by Zahedinejad et al. [38] is solved by means of the differential quadrature method.

Conclusions

The present work proposes the 3D equilibrium equations developed in general orthogonal curvilinear coordinates for the free vibration analysis of single-layered and sandwich plates, cylinders and spherical/cylindrical shell panels embedding FGM layers. The system of second-order differential equations has been reduced in a system of first-order differential equations redoubling the variables. Therefore, the obtained system of differential equations has been solved by means of the

exponential matrix method. The solution has been proposed in closed-form considering simply supported structures and harmonic displacement components. The equilibrium equations have variable coefficients because of variable elastic coefficients in z for FGMs and/or parametric coefficients including radii of curvature and coordinate z for shell geometries. A number M of mathematical layers has been introduced to correctly approximate both elastic coefficients and parametric terms and to correctly solve the 3D equations with variable coefficients. When the opportune value for M is identified, an appropriate order N for the exponential matrix must be chosen in order to solve the differential equations. The exponential matrix method has a very fast convergence ratio and it is very stable. Small values for N can be used when a big value for M is employed. The choice of the opportune M value depends on the geometry (in particular the thickness) and even more on the FGM law (complicated through-the-thickness FGM laws require higher M values). In conclusion, the opportune N and M values depend on several parameters such as geometry, thickness ratio, material, lamination sequence, FGM law, imposed half-wave numbers, frequency orders, and vibration mode. In order to obtain correct results and a high reliability and stability of the method, the choice of $M = 100$ combined with $N = 3$ appears as the best possible combination for all the proposed cases.

Declaration of Conflicting Interests

The author(s) declared no potential conflicts of interest with respect to the research, authorship, and/or publication of this article.

Funding

The author(s) received no financial support for the research, authorship, and/or publication of this article.

References

1. Birman V and Byrd LW. Modeling and analysis of functionally graded materials and structures. *Appl Mech Rev* 2007; 60: 195–216.
2. Dong L and Atluri SN. A simple procedure to develop efficient & stable hybrid/mixed elements, and Voronoi cell finite elements for macro- & micro-mechanics. *CMC* 2011; 24: 61–104.
3. Bishay PL, Sladek J, Sladek V, et al. Analysis of functionally graded magneto-electro-elastic composites using hybrid/mixed finite elements and node-wise material properties. *CMC* 2012; 29: 213–262.
4. Bishay PL and Atluri SN. High-performance 3D hybrid/mixed, and simple 3D Voronoi cell finite elements, for macro- & micro-mechanical modeling of solids, without using multi-field variational principles. *CMES* 2012; 84: 41–97.
5. Brischetto S. Classical and mixed advanced models for sandwich plates embedding functionally graded cores. *J Mech Mater Struct* 2009; 4: 13–33.
6. Brischetto S and Carrera E. Advanced mixed theories for bending analysis of functionally graded plates. *Comput Struct* 2010; 88: 1474–1483.

7. Brischetto S, Leetsch R, Carrera E, et al. Thermo-mechanical bending of functionally graded plates. *J Therm Stress* 2008; 31: 286–308.
8. Mattei G, Tirella A and Ahluwalia A. Functionally Graded Materials (FGMs) with predictable and controlled gradient profiles: Computational modelling and realisation. *CMES* 2012; 87: 483–504.
9. Tornabene F and Fantuzzi N. *Mechanics of laminated composite doubly-curved shell structures. The generalized differential quadrature method and the strong formulation finite element method*. Bologna, Italy: Società Editrice Esculapio, 2014.
10. Tornabene F. *Meccanica delle Strutture a Guscio in Materiale Composito*. Bologna, Italy: Società Editrice Esculapio, 2012.
11. Reddy JN. *Mechanics of laminated composite plates and shells: Theory and analysis*, 2nd ed. New York: CRC Press, 2004.
12. Carrera E, Brischetto S and Nali P. *Plates and shells for smart structures: Classical and advanced theories for modeling and analysis*. New Delhi: John Wiley & Sons, Ltd., 2011.
13. Gustafson GB. Systems of differential equations, http://www.math.utah.edu/gustafso/2250systems-de.pdf (accessed 7 March 2016).
14. Boyce WE and DiPrima RC. *Elementary differential equations and boundary value problems*. New York: John Wiley & Sons, Ltd, 2001.
15. Zwillinger D. *Handbook of differential equations*. New York: Academic Press, 1997.
16. Molery C and Van Loan C. Nineteen dubious ways to compute the exponential of a matrix, twenty-five years later. *SIAM Rev* 2003; 45: 1–46.
17. Brischetto S. Exact elasticity solution for natural frequencies of functionally graded simply-supported structures. *CMES* 2013; 95: 391–430.
18. Brischetto S. Three-dimensional exact free vibration analysis of spherical, cylindrical, and flat one-layered panels. *Shock Vib* 2014; 2014. Article ID 479738, 1–29.
19. Brischetto S. An exact 3D solution for free vibrations of multilayered cross-ply composite and sandwich plates and shells. *Int J Appl Mech* 2014; 6: 1–42.
20. Brischetto S. A continuum elastic three-dimensional model for natural frequencies of single-walled carbon nanotubes. *Compos Part B: Eng* 2014; 61: 222–228.
21. Brischetto S. A continuum shell model including van der Waals interaction for free vibrations of double-walled carbon nanotubes. *CMES* 2015; 104: 305–327.
22. Brischetto S and Torre R. Exact 3D solutions and finite element 2D models for free vibration analysis of plates and cylinders. *Curved Layer Struct* 2014; 1: 59–92.
23. Tornabene F, Brischetto S, Fantuzzi N, et al. Numerical and exact models for free vibration analysis of cylindrical and spherical shell panels. *Compos Part B: Eng* 2015; 81: 231–250.
24. Brischetto S, Tornabene F, Fantuzzi N, et al. 3D exact and 2D generalized differential quadrature models for free vibration analysis of functionally graded plates and cylinders. *Meccanica* 2016.
25. Brischetto S, Tornabene F, Fantuzzi N, et al. Refined 2D and exact 3D shell models for the free vibration analysis of single- and double-walled carbon nanotubes. *Technologies* 2015; 3: 259–284.
26. Messina A. Three dimensional free vibration analysis of cross-ply laminated plates through 2D and exact models. In: *3rd international conference on integrity, reliability and failure*, Porto, Portugal, July 2009, pp. 20–24.
27. Soldatos KP and Ye J. Axisymmetric static and dynamic analysis of laminated hollow cylinders composed of monoclinic elastic layers. *J Sound Vib* 1995; 184: 245–259.

28. Dong CY. Three-dimensional free vibration analysis of functionally graded annular plates using the Chebyshev-Ritz method. *Mater Des* 2008; 29: 1518–1525.
29. Li Q, Iu VP and Kou KP. Three-dimensional vibration analysis of functionally graded material sandwich plates. *J Sound Vib* 2008; 311: 498–515.
30. Malekzadeh P. Three-dimensional free vibration analysis of thick functionally graded plates on elastic foundations. *Compos Struct* 2009; 89: 367–373.
31. Hosseini-Hashemi S, Salehipour H and Atashipour SR. Exact three-dimensional free vibration analysis of thick homogeneous plates coated by a functionally graded layer. *Acta Mech* 2012; 223: 2153–2166.
32. Vel SS and Batra RC. Three-dimensional exact solution for the vibration of functionally graded rectangular plates. *J Sound Vib* 2004; 272: 703–730.
33. Kashtalyan M. Three-dimensional elasticity solution for bending of functionally graded rectangular plates. *Eur J Mech A/Solids* 2004; 23: 853–864.
34. Xu Y and Zhou D. Three-dimensional elasticity solution of functionally graded rectangular plates with variable thickness. *Compos Struct* 2009; 91: 56–65.
35. Kashtalyan M and Menshykova M. Three-dimensional elasticity solution for sandwich panels with a functionally graded core. *Compos Struct* 2009; 87: 36–43.
36. Zhong Z and Shang ET. Three-dimensional exact analysis of a simply supported functionally gradient piezoelectric plate. *Int J Solids Struct* 2003; 40: 5335–5352.
37. Alibeigloo A, Kani AM and Pashaei M-H. Elasticity solution for the free vibration analysis of functionally graded cylindrical shell bonded to thin piezoelectric layers. *Int J Press Vess Pip* 2012; 89: 98–111.
38. Zahedinejad P, Malekzadeh P, Farid M, et al. A semi-analytical three-dimensional free vibration analysis of functionally graded curved panels. *Int J Press Vess Pip* 2010; 87: 470–480.
39. Chen WQ, Bian ZG and Ding HJ. Three-dimensional vibration analysis of fluid-filled orthotropic FGM cylindrical shells. *Int J Mech Sci* 2004; 46: 159–171.
40. Vel SS. Exact elasticity solution for the vibration of functionally graded anisotropic cylindrical shells. *Compos Struct* 2010; 92: 2712–2727.
41. Sladek J, Sladek V, Krivacek J, et al. Meshless local Petrov-Galerkin method for stress and crack analysis in 3-D axisymmetric FGM bodies. *CMES* 2005; 8: 259–270.
42. Sladek J, Sladek V, Tan CL, et al. Analysis of transient heat conduction in 3D anisotropic functionally graded solids, by the MLPG method. *CMES* 2008; 32: 161–174.
43. Sladek J, Sladek V and Solek P. Elastic analysis in 3D anisotropic functionally graded solids by the MLPG. *CMES* 2009; 43: 223–252.
44. Hildebrand FB, Reissner E and Thomas GB. *Notes on the foundations of the theory of small displacements of orthotropic shells*. NACA Technical Note No. 1833, Washington, 1949.
45. Soedel W. *Vibration of shells and plates*. New York: Marcel Dekker, Inc., 2004.